Science
AAAS

Supplementary Materials for

Genetic excision of the regulatory cardiac troponin I extension in high–heart rate mammal clades

William Joyce *et al*.

Corresponding authors: William Joyce, william.joyce@bio.au.dk; Kevin L. Campbell, kevin.campbell@umanitoba.ca

Science **385**, 1466 (2024)
DOI: 10.1126/science.adi8146

The PDF file includes:

Materials and Methods
Figs. S1 to S13
Tables S1 to S4
References

Other Supplementary Material for this manuscript includes the following:

MDAR Reproducibility Checklist
Data S1 to S4

Supplementary Materials

Materials and Methods

1. Experimental subject details

For protein and mRNA expression studies we acquired heart tissue from the most diverse range of eulipotyphlans available. Samples were either obtained opportunistically from already deceased specimens or captured with appropriate regional permits (see table S3 for details). DNA sequencing was also performed on archived liver samples from three talpid species provided by collaborators and/or collected for other studies (38, 39). Two greater roundleadf bats (*Hipposideros armiger*), selected because publicly available RNA-seq data (see below) indicated cTnI alternative splicing in this species, were obtained following local government permit and university ethical committee approval (table S3). Laboratory mice hearts were obtained with relevant institutional ethical approvals and following institutional regulations (table S3).

2. *TNNI3*/cTnI nucleotide/protein sequences

2.1 Gene predictions and genome annotation

Gnomon-predicted *TNNI3* coding sequences from three eulipotyphlan species (*Sorex araneus*, *Condylura cristata*, and *Erinaceus europaeus*) were first retrieved from National Center for Biotechnology Information (NCBI) GenBank using key word searches and the *TNNI3* ortholog page (https://www.ncbi.nlm.nih.gov/gene/7137/ortholog/?scope=9362&term=TNNI3). As the *C. cristata* sequence (GB accession number XM_004694091.2) was found to be mis-annotated, the contig housing the gene (AJFV01074313.1) was downloaded and manually annotated. The resulting coding sequences were used as nucleotide blast (blastn) (*82*) queries against eulipotyphlan whole-genome shotgun sequences using the "discontinuous megablast" setting. Contigs returned as hits were downloaded and annotated using the Geneious (version 9.1.8) annotate function. In cases where gaps in coding sequence were apparent (for example *Uropsilus nivatus, Crocidura indochinensis*) or for sequenced species for which whole-genome shotgun sequences were unavailable (*Neohylomys hainanensis*), corresponding regions from closely related species were used as blastn queries against sequence read archive (SRA) files. All hits were downloaded and assembled to coding regions of closely related species using the Geneious map to reference function. As only raw (unassembled) genomic data were available for *S. fumeus* (SRR18739258), SRA files for this species were first converted to fastq sequence reads using the *fastq-dump* function in the SRA-Toolkit v3.0.0 (NCBI). Fastq reads were trimmed of adapter and low-quality sequences using BBDuk (Joint Genomics Institute) with the flags mink=11, hdist=1, tpe, tbo, qtrim=rl and timq=10. Trimmed reads were assembled to a *TNNI3* reference sequence (*Sorex palustris*) using BBMap (Joint Genomics Institute) with the flags maxindel=80 and k=10. All mined data were imported to Geneious and annotated as above. Linear sequence comparison figures of the genomic data were prepared using EasyFig (*83*).

2.2 Transcriptomics and mRNA sequencing

Heart samples collected from 13 eulipotyphlan species were placed in RNAlater (Qiagen, China) and stored at -80°C. Total RNA was extracted from each specimen and *de novo* assembled transcriptomes were generated using Trinity v2.4.1. with default parameters as previously

described (*38*). The species list and source of tissues for mRNA extraction are provided in table S3.

Total mRNA was also extracted from ~60 mg of heart tissue of five eulipotyphlan species (table S3) using Trizol (Invitrogen) following the manufacturer's instructions. cDNA was generated with SMARTScribe Reverse Transcriptase (Takara) or ProtoScript II Reverse Transcriptase (NEB) according to the manufacture's recommendations. PCRs were performed using Phusion DNA Polymerase with GC buffer supplemented with 3% DMSO. Thermocycling conditions followed the manufacture's recommendations, with the exception of annealing temperature and cycle count, which was optimised for each primer pair (table S4). Primers were designed from the predicted *TNNI3* sequences for a given species or closest available phylogenetic relatives. Amplicons of the expected size (~600 bp) were extracted from a 1.2% agarose gel in 1X SB Buffer and purified using GENEJet Gel Extraction Kit (Thermo Scientific). PCRs yielding non-specific amplification products were used as template in a nested PCR, using the primers defined in table S4, and then purified as above. Purified PCR amplicons were sequenced in both directions using the amplification primers by either Eurofins Genomics or the Toronto Sick Kids Centre for Applied Genomics. All new sequences have been deposited in GenBank (see accession numbers in data S1).

Publicly deposited heart transcriptome SRA data from 11 chiropteran and five additional eulipotyphlan species (see table S1) were also downloaded to Geneious and assembled to both *TNNI3* and *TNNI1* coding sequences that we annotated for these same or closely related species using the "Map to Reference" function. To test for alternative exon 3 splicing in the 12 species with intact exon 3 sequences, SRA reads were first assembled to manually modified mRNA transcripts lacking exon 3. The resulting assemblies failed to provide evidence for alternative exon 3 splicing in both erinaceid (*Atelerix albiventris*) heart transcriptomes, though provided unequivocal evidence for alternative exon 3 splicing in all 10 available *Artibeus*, *Hipposideros*, and *Rhinolophus* specimens. To estimate the relative expression levels of alternatively spliced (lacking exon 3) and full-length (possessing exon 3) *TNN13* transcripts for the latter 10 bat specimens, 66 bp contigs (containing only exons 1, 2 and 4, and only exons 1, 2 and 42 bp of exon 3, respectively) were first constructed and used as templates for the SRA assemblies (maximum 5% mismatch threshold for both). A similar strategy was used to estimate the relative expression levels of *TNNI1* and *TNNI3* for the above 16 species, whereby coding sequences of *TNNI1* exons 3-7 and *TNNI3* 4-8 were used as templates for the SRA assemblies (maximum 10% mismatch threshold for both). All assemblies were visually inspected to ensure negligible off-target sequences were incorporated into the assemblies.

2.3 PCR of exon 3 region

As sequence data spanning the exon 3 region of *TNNI3* were unavailable for one of the major mole clades (shrew moles), we used previously extracted *Urotrichus talpoides* DNA (SIK207) to PCR amplify this region. Primers (table S4) in the upstream UTR and exon 4 were designed from known mRNA (transcriptome) sequences of this species. A similar strategy was employed to target this region from previously extracted *Uropsilus gracilis* DNA. Primers designed from the upstream UTR and exon 5 of the Pyrenean desman were also used to amplify the N-terminal region from previously purified Russian desman (*Desmana moschata*) DNA (*38, 39*). PCRs were performed, and the resulting amplicons (700-1100 bp) were purified and sequenced as described in 2.2.

2.4 Selection analyses

Selection analyses were performed with the codeml program in PAML 4.9 (*46*) and the RELAX program (*47*) of HyPhy (*84*). Analyses were performed with (a) complete protein-coding sequences of the *TNNI3* gene (except for exon 3) for 48 placental mammal taxa (codeml and RELAX) and (b) exon 3 sequences for a reduced data set with 32 taxa that did not include shrews (RELAX only as codeml failed to return results; see data S2). The 48 placental mammal taxa include representatives from all four placental superorders (Afrotheria, Xenarthra, Laurasiatheria, and Euarchontoglires), but have enriched sampling within Laurasiatheria (data S1). Analyses with codeml were performed with two different codon frequency models, CodonFreq = 1 and CodonFreq = 2. We used cleandata = 0 (sites with ambiguity data were not removed) and method = 0 (dN/dS [=ω] values were estimated simultaneously across the tree). First, we compared a model with one dN/dS category for all branches to a model with two dN/dS branch categories for the protein-coding sequence alignment that included exons 1, 2, and 4-8. (dN/dS is the ratio of nonsynonymous to synonymous substitution rates.) In the two-category branch model, the first category was for branches leading to taxa with an intact copy of the coding sequence for exon 3 and the second category was for branches with one or more inactivating mutations in exon 3 (crown *Talpa* + stem *Talpa* + *Condylura* + *Urotrichus* + crown *Uropsilus* + stem *Uropsilus* + crown Soricidae + stem Soricidae). We performed these analyses to determine if exons 1, 2, and 4-8 have remained under purifying selection in taxa with a pseudoexonic copy of exon 3. We used the chi2 program in PAML to perform a log-likelihood ratio test on models with one versus two branch categories. We also performed an analysis with nine different branch categories (background + crown *Talpa* + stem *Talpa* + *Condylura* + *Urotrichus* + crown *Uropsilus* + stem *Uropsilus* + crown Soricidae + stem Soricidae) to ascertain the range of dN/dS values on branches of the tree that are transitional or fully pseudoexonic (*sensu* (*85*)) for exon 3. Analyses with RELAX were performed with two different models. The first model (RELAX null) allowed for a single branch category. The second model (RELAX alternative) allowed for two branch categories: foreground (Test), background (Reference). Both models allowed for three different ω values within each branch category (ω_1, ω_2, ω_3). Comparisons between the alternative and null models were performed with lnL ratio tests in RELAX (*47*). For the analysis with 48 complete coding sequences (minus exon 3), the foreground branch category included all branches that are transitional or fully pseudoexonic for exon 3, and the background branch category included all of the remaining branches. For exon 3, the data set included 32 taxa and we performed two analyses. In the first analysis, the foreground category included branches for six non-desman talpids (*Condylura cristata, Scalopus aquaticus, Talpa occidentalis, Uropsilus gracilis, Uropsilus nivatus, Urotrichus talpoides*) and the stem branch for *Uropsilus*, all of which have inactivating mutations for exon 3. All of the non-talpid branches were assigned to the background branch category and all of the remaining talpid branches were left as unclassified and therefore ignored in the ω calculations and statistical tests. In the second analysis, both desmans (*Galemys pyrenaicus* and *Desmana moschata*) and the stem desman branch were assigned to the foreground branch category (both desmans have intact copies of exon 3). All of the remaining talpid branches were left as unclassified and all non-talpid branches were assigned to the background branch category. We performed this test to determine if the exon 3 sequences in the desmans have evolved under relaxed selection relative to other mammals even though the exon sequences remain intact. For both of the analyses with 32 taxa, premature stop codons were replaced with Ns, frameshift insertions were deleted, and frameshift deletions were filled in with Ns (frameshift deletions) in talpid taxa with inactivating mutations.

2.5 Phosphorylation site scores

Phosphorylation site scoring was performed using the NetPhos 3.1 (*48*) online server (https://services.healthtech.dtu.dk/services/NetPhos-3.1/). cTnI protein sequence for *G. pyrenaicus* (including the predicted peptide encoded by exon 3) were uploaded along with *E. europaeus, M. musculus and H. sapiens* sequences. PKA phosphorylation site scores were recorded for $Ser_{23/24}$ for all species. Scores above 0.500 are 'positive' indicating a residue is a target for a given kinase.

2.6 Splice site likelihood modelling

To investigate the potential for alternative splicing in desmans (*G. pyrenaicus* and *D. moschata*; these species have intact splice sites and, unlike other moles and shrews, no inactivating indels), we performed maximum entropy analysis of 3' and 5' splice site strength (*49*). For each exon, the 3' splice site strength analysis was performed at the 3' end of the preceding (upstream) intron and the 5' splice site analysis was performed with the 5' end of the subsequent (downstream) intron (*50*). We compared the desmans with several representative species in our study that also have intact exon 3 splice sites and no indels (*Homo sapiens*, human; *Mus musculus*, house mouse; *Solenodon paradoxus*, Hispaniolan solenodon; *Erinaceus europaeus*, European hedgehog; *Neohylomys hainanensis*, Hainan gymnure). Two bat species shown to exhibit alternative exon 3 splicing (*Hipposideros armiger*, great roundleaf bat; *Artibeus jamaicensis*, Jamaican fruit bat) were also included in this analysis. Calculations were performed using the server hosted on the Burge Lab website (http://hollywood.mit.edu/burgelab/maxent/Xmaxentscan_scoreseq_acc.html). Because this analysis is optimized for comparison with the human genome, we also made equivalent comparisons for the neighboring exons (exons 2 and 4) in *TNNI3* for each species to ensure that the output yielded consistent comparisons across species.

3. Protein expression characterisation

3.1 Western blotting

The species list and source of tissues are provided in table S3. Previous work has shown that although cardiac troponin I gradually degrades after death, producing lower molecular weight fragments, an intact cTnI band remains visible in western blots from mammalian heart tissues collected up to at least four days post mortem (*86*). Thus, hearts from several free-ranging species that were opportunistically collected within this timeframe were included in these experiments. Note that post-mortem times of <24 h were verified in all species except the greater white-toothed shrew, *Crocidura russula*, for which time of death was unknown but estimated to be 24 to 72 h. To confirm that both exon 3^+ and exon 3^- cTnI isoforms were incorporated into cardiac myofilaments, myofibrillar proteins were also isolated for the house mouse (*Mus musculus*), great roundleaf bat (*Hipposideros armiger*; 2 specimens), Asian house shrew (*Suncus murinus*), and Chinese mole shrew (*Anourosorex squamipes*) using a previously published protocol (*87*).

Protein extraction was performed by homogenization of cardiac ventricular tissues in RIPA buffer (ThermoFisher 89900 or Beyotime P0013B) with 1% protease and phosphatase inhibitor (PPI) cocktail (Sigma-Aldrich PPC1010 or Beyotime P1045). Protein concentration was measured with bicinchoninic acid (BCA) assay (Millipore 71285-3 or Sangon C503021-

0500) and samples were diluted to 2 µg protein μl^{-1} with RIPA buffer and PPIs, and were then denatured with an equal volume of 2x Laemmli buffer (Sigma-Aldrich S3401) and heating to 95°C for 5 min.

Proteins were separated using sodium dodecyl sulfate–polyacrylamide gel electrophoresis (SDS-PAGE). Samples were loaded (15 µg protein per lane) alongside protein ladders (5 µl per lane, BLUeye Prestained Protein Ladder, Sigma-Aldrich 94964) on tris-glycine gels (16% acrylamide 1.0 mm, ThermoFisher XP00165BOX or XP00160BOX) using an Invitrogen XCell SureLock Mini-Cell or a SINSAGE-PR2. Proteins were thereafter transferred to a PVDF membrane (Invitrolon PVDF/Filter Paper Sandwiches, 0.45 µm, ThermoFisher LC2005 or Beyotime FFP36) with an XCell II Blot Module or a SINSAGE-BLOT2. Total protein loading was visualised with No-Stain™ Protein Labeling Reagent (ThermoFisher A44717) following the manufacturer's instructions and imaged on a Bio-Rad ChemiDoc. Subsequently, blocking was performed for 1 h at room temperature with 5% skim milk in tris-buffered saline with 0.05% Tween 20 (TBS-T).

cTnI western blotting was achieved with a mouse monoclonal primary antibody against troponin I (Santa-Cruz SC-133117, 1:1000 dilutions of the 200 µg ml^{-1} stock) diluted in 2% skim milk in TBS-T which was incubated with the blot overnight at 4°C or for 1 h at room temperature. After washing with TBS-T, a HRP-conjugated anti-mouse secondary antibody (Santa-Cruz sc-516102, 1:5000 dilution of 400 µg ml^{-1} stock) in 2% skim milk TBS-T was used for a 1 h incubation at room temperature. Blots were imaged on a Bio-Rad ChemiDoc and chemiluminescent signals were developed with Millipore/Immobilon Classico Western HRP substrate (Merck WBLUC0500). Densitometric analysis was performed using IOCBIO Gel (*88*).

We also compared protein kinase A (PKA) phosphorylated proteins after exogenous PKA treatment. The exogenous treatment was designed to account for rapid post mortem decay of native phosphorylation (*89*), which would otherwise have precluded comparisons between samples. One protein extract (40 µg per 50 µl reaction) from each species (mouse, West European hedgehog, greater white-toothed shrew, European pygmy shrew, Pyrenean desman, and European mole) was incubated with catalytic subunit of PKA (5 µl per reaction, New England Biolabs P6000SVIAL) in NEBuffer™ for Protein Kinases (New England Biolabs B6022SVIAL) with 200 µM adenosine triphosphate (New England Biolabs P0756S). The treatment was performed for 1 h at 30°C and was terminated by addition of an equal volume of 2x Laemmli buffer (Sigma-Aldrich S3401) and heating to 95°C for 5 min. SDS-PAGE and western blotting was performed as described above, except 8 µg protein per lane was loaded. Antibodies designed to specifically detect N-terminal phosphorylated cTnI ($Ser_{23/24}$ in the region encoded by exon 3; Cell Signaling 4004S, rabbit primary antibody, 1:1000 dilution of unspecified stock concentration) or general phosphorylated protein kinase A (phospho-PKA) substrates (RRXS*/T*; New England Biolabs 9624S rabbit primary antibody, 1:1000 dilution of unspecified stock concentration). Incubation was performed for 1 h at room temperature or 4°C overnight on shaker, respectively. This was followed by incubation with a HRP-conjugated goat anti-rabbit secondary antibody (New England Biolabs 7074P2; 1:3000 dilution of unspecified stock concentration) for 1 h at room temperature. The blot was imaged as described above, then stripped using Restore Western Blot Stripping Buffer (ThermoFisher 21059) and the TnI antibody protocol was followed as described above.

3.2 Ectopic expression of exon 3^+ and exon 3^- desman cTnI proteins for western blot analysis

Expression cassette construction. Coding sequences encoding *Galemys pyrenaicus* cTnI proteins, both with and without exon 3, were optimized for expression in *E. coli* and synthesized in vitro by GeneArt (Regensburg, Germany). Gene cassettes were ligated into a custom expression vector (*90*) using a New England BioLabs Quick Ligation Kit as recommended by the manufacturer. Chemically competent JM109 (DE3) *E. coli* (Promega) were prepared using a Z-Competent *E. coli* Transformation Kit and Buffer Set (Zymo Research). cTnI expression vectors were transformed into JM109 (DE3) chemically competent *E. coli* according to manufacturer's recommendations, plated on LB agar containing ampicillin (100 µg/ml), and incubated for 18 h at 37°C. A single colony from each transformation was cultured in 50 ml of LB broth for 16 h at 37°C on an orbital shaker at 200 rpm. Post incubation, 5 ml of the culture was pelleted by centrifugation and plasmid DNA was isolated using a GeneJET Plasmid Miniprep Kit (Thermo Scientific). The plasmid sequence was verified by Sanger sequencing at The Centre for Applied Genomics (Toronto, Ontario). The remainder of the culture was supplemented with glycerol to a final concentration of 10% and stored at –80°C until needed for expression.

Protein expression. 45 ml of starter culture (above) was added to 2500 ml of TB medium containing ampicillin (100 µg/µl) and Antifoam SE-15 (0.1%; Sigma) in a 3 L spinner flask. Cultures were grown in a circulating water bath at 37°C, stirred with a cross blade impeller at 800 rpm and supplemented with air (0.08 l/min). Growth was monitored until the culture absorbance at 600 nm reached 0.6–0.8. Expression was then induced by supplementing the media with 0.2 mM isopropyl β-D-1-thiogalactopyranoside and 20 g/L of glucose. The culture was incubated at 28°C for 16 h and then cells were pelleted by centrifugation at 5000 x g for 10 min.

Cell lysis. Cell pellets were re-suspended in cell lysis buffer (33 mM Tris-HCl, 0.5 mM DTT; 3 ml per gram cell paste), supplemented with lysozyme (1 mg per gram cell paste) and mixed in an orbital shaker at 300 rpm for 20 min at 20°C. Samples were sonicated on ice using a Fisher Scientific model 705 sonic dismembrator at 32 W with 10 seconds on/20 seconds off cycles for 15 min. TnI protein expression was visualized with western blotting as described above.

3.3. Immunoprecipitation and LC-MS/MS analysis of the 22 kDa *TNNI3* protein from desman and shrew heart lysates

To verify that the 22 kDa band corresponded to cTnI (as opposed to the product of another *TNNI* gene paralog), we immunoprecipitated the TnI proteins of Pyrenean desman (*Galemys pyrenaicus*) and northern short-tailed shrew (*Blarina brevicauda*) hearts using the anti-Troponin I (C-4) (sc-133117, Santa Cruz). Briefly, a 30 µl slurry of protein G-Sepharose beads (Pierce) was washed three times with 500 µl of RIPA buffer (50 mM Tris-HCl, pH 7.6, 150 mM NaCl, 1% Triton X-100, 0.5% deoxycholic acid, 0.1% SDS), and resuspended in 30 µl of PBS buffer (MP Biomedicals). The beads were then incubated with 1.3 µl of the anti-Troponin I antibody and 100 µl of protein lysate at 4°C for 3 h with rotation, and then washed three times each with 500 µl of RIPA buffer followed by elution with 15 µl of glycine buffer (0.15 M NaCl, 0.2 M glycine-HCl, pH 2.0) on ice for 5 min. The eluted proteins were denatured in SDS protein loading buffer at 95°C for 5 min and resolved in 4-20% SDS-polyacrylamide gradient gels. The gel was stained with Coomassie brilliant blue G250 for 1 h, de-stained with 10% acetic acid, and the ~22 kDa band was visualized above a fluorescent light box and excised using a clean glass coverslip. Before mass spectrometry, the identity of the ~22 kDa bands were confirmed by western blot analysis using the anti-Troponin I antibody in a separate test. The *TNNI3* 22kDa

bands were sent for LC-MS/MS mass spectrometry analysis at the Southern Alberta Mass Spectrometry (SAMS) Centre, University of Calgary. As protein coding sequences for both *TNNI1* (encoding ssTnI) and *TNNI3* (encoding cTnI) of these two species are either unavailable or misannotated on GenBank, they were provided to the SAMS facility and included in the resulting in-house analysis.

3.4. Immunoprecipitation and targeted LC-MS/MS analysis of the 22 kDa *TNNI3* protein from bat and shrew heart lysates

Given that standard LC-MS/MS for protein identification (above) was unable to recover the *TNNI3* exon 2/exon 4 splicing boundary, we performed LC-MS/MS with parallel reaction monitoring to target the N-terminal region of the great roundleaf bat (*Hipposideros armiger*) and Asian house shrew (*Suncus murinus*). Heart lysates were immunoprecipitated similar to that described above, with the exception that we used 13 µl of primary antibody and 150 µl of protein lysate. The excised ~22 kDa bands were sent to Wininovate Bio (Guangzhou, China) for sequencing and the MS/MS data were analyzed with PEAKS Studio 8.5 (Bioinformatics Solutions Inc., Waterloo, Canada) with a local false discovery rate at peptide-spectrum matches as 1.0% after searching against target sequences database with a maximum of three missed cleavages. Acetylation (Protein N-term) were selected for variable modifications. Precursor and fragment mass tolerance were set to 10 ppm and 0.05 Da, respectively.

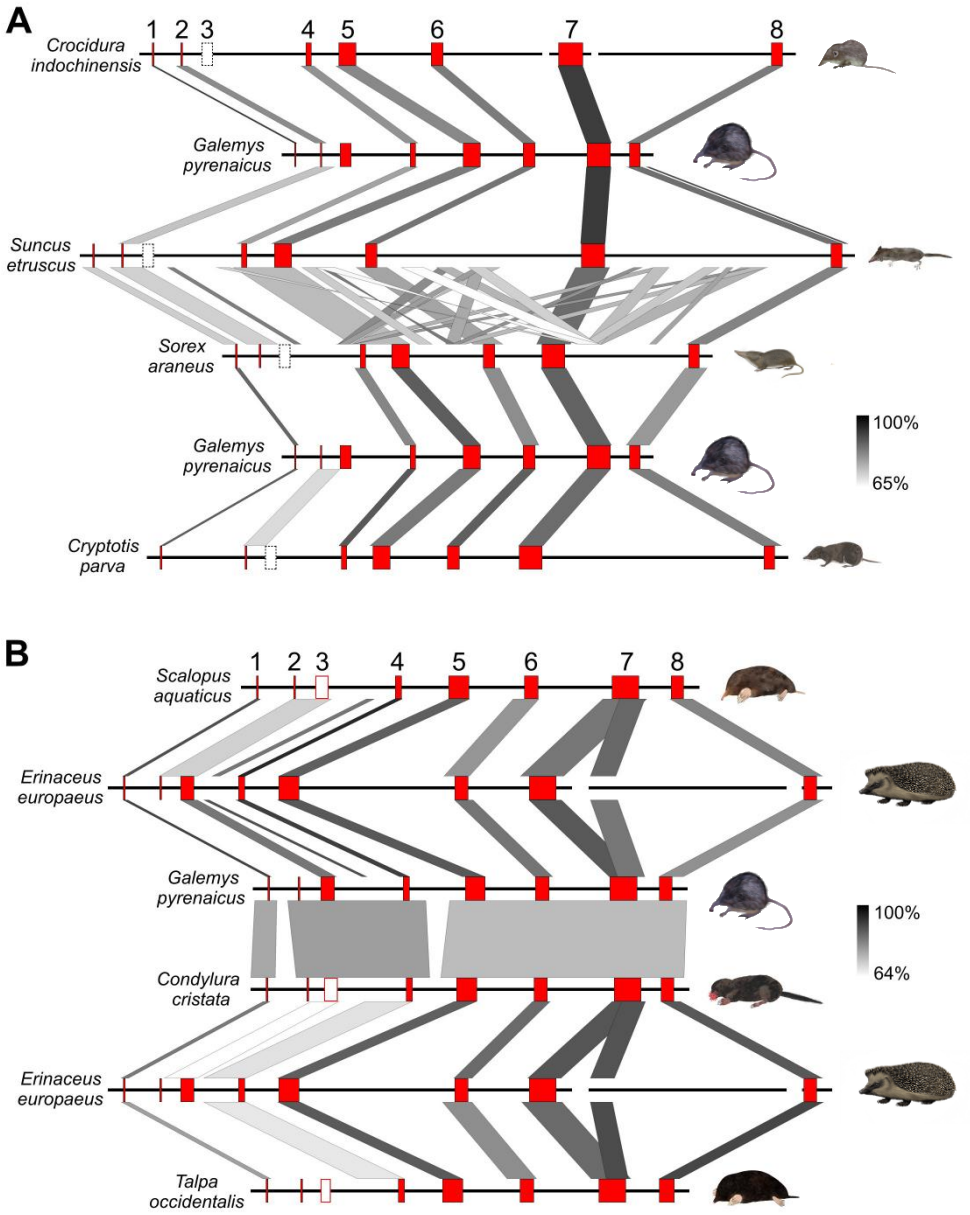

Figure S1. Sequence identity comparisons of the *TNNI3* gene of select eulipotyphlan mammals. (A) Linear comparisons illustrating the deletion of exon 3 (expected location denoted by open dashed boxes) in the genomes of four shrew species relative to the Pyrenean desman (*Galemys pyrenaicus*). B) Linear comparisons of four talpid mole species relative to the European hedgehog (*Erinaceus europaeus*). Intact exons are numbered and highlighted in red, while pseudoexonized (non-coding) exon 3 of moles is denoted by red open boxes. Thick black horizontal lines represent intron sequences while gaps denote missing data. Note that the sequence identity of the intact coding exons of moles (1, 2, 4-8) relative to corresponding coding exons of the hedgehog are higher than that of the non-coding exon 3 of moles, except for the Pyrenean desman whose intact exon 3 retains a relatively high sequence conservation.

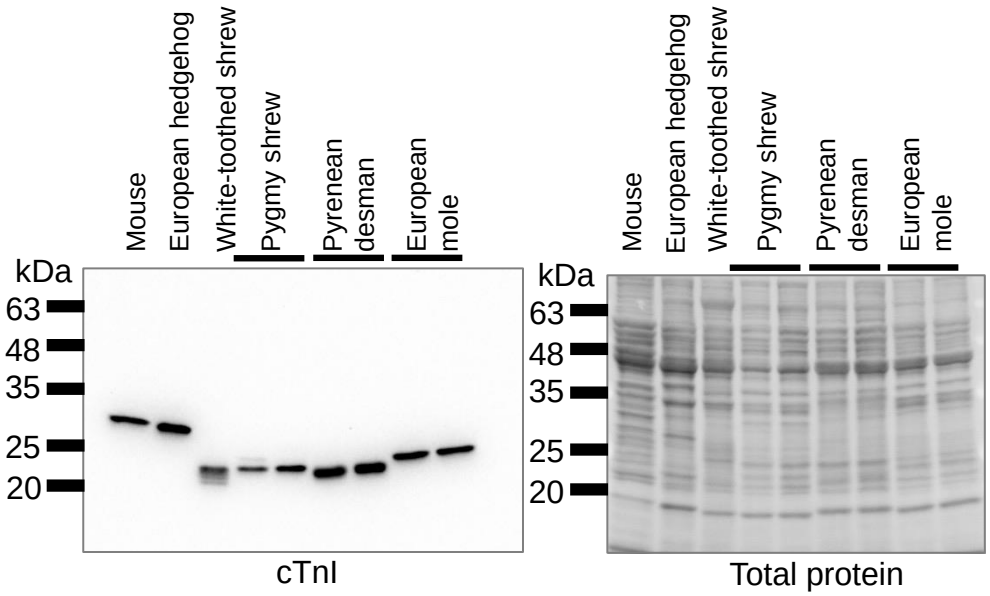

Figure S2. Cardiac troponin I (cTnI) expression in heart extracts from representative eulipotyphlan species and mouse. cTnI western blotting including two individuals of pygmy shrew, two of five Pyrenean desmans (see fig. S10 for all five), and two European moles. Note that the marginally higher molecular mass in European mole than the shrew and desman cTnI is attributable to a four amino acid extension at the C-terminus (see fig. S13; data S1). Total protein was visualised with No-Stain Protein Labeling Reagent.

Blarina brevicauda

Peptide matches to *Blarina* cTnI: **6 matches (4 non-duplicate, 2 duplicate)**

Hit	Start-end	Observed mass	Expected mass	Calculated mass	Ion score	Expect value	Rank order	Peptide
1	23-30	467.2777	932.5408	932.5365	26	0.0025	1	K.TLMLQIAK.Q + Oxidation (M)
2	93-103	609.3216	1216.6286	1216.6299	35	0.00031	1	K.NVSEIADLTQK.V
3	121-134	755.3737	1508.7328	1508.7327	15	0.321	1	R.ISADAMMQALLGTR.A + 2 Oxidation (M)
4	121-134	755.3737	1508.7328	1508.7327	77	1.8e-08	1	R.ISADAMMQALLGTR.A + 2 Oxidation (M)
5	121-134	755.3737	1508.7328	1508.7327	58	1.4e-06	1	R.ISADAMMQALLGTR.A + 2 Oxidation (M)
6	168-178	589.7769	1177.5392	1177.5397	15	0.034	1	K.NIDALSGMEGR.K + Oxidation (M)

>*Blarina brevicauda TNNI3* (cTnI)
MADERGAAKKSKITASRKLQLK**TLMLQIAK**QELEREVEERRGEKGRALSARCQPLELAGLGFAELQDLCRQLHAQ
VDKVDEERYDVEAKVTK**NVSEIADLTQK**VIDLRGKFKRPTLRRVR**ISADAMMQALLGTR**AKESLDLRANLKQVKK
EDTEKVKENREVGDWRK**NIDALSGMEGR**KKKFEG

Peptide matches to *Blarina* ssTnI: **none**

>*Blarina brevicauda TNNI1* (ssTnI)
MPEVERKSKITASRKLLLKSLMLAKAKECWEQEHEEREAEKARYLAERIPTLQTRGLSLSALQDLCRDLHAQVEV
VDEERYDIEAKCLHNTREIKDLKLKVLDLRGKFKRPPLRRVRVSADAMLRALLGSKHKVSMDLRANLKSVKKEDT
EKERPVEVGDWRKNVEAMSGMEGRKKMFDAAKTPVTQ

Galemys pyrenaicus

Peptide matches to *Galemys* cTnI: **2 matches (2 non-duplicate, 0 duplicate)**

Hit	Start-end	Observed mass	Expected mass	Calculated mass	Ion score	Expect value	Rank order	Peptide
1	93-103	609.3210	1216.6274	1216.6299	16	0.022	1	K.NVSEIADLTQK.V
2	166-176	589.7759	1177.5372	1177.5397	13	0.047	1	K.NIDALSGMEGR.K + Oxidation (M)

>*Galemys pyrenaicus TNNI3* (cTnI)
MADESREAKKSKISASRKLQLKTLMLQVAKQELEREAEERRGEKGRALSARCEPLELARLGFAELQDLCRQLHAR
VDKVDEERYDVEAKVTK**NVSEIADLTQK**ILDLRGKFKRPALRRVRISADAMMQALLGTRAKESMDLRANLKQVKK
EDTEKENREVGDWRK**NIDALSGMEGR**KKKFEG

Peptide matches to *Galemys* ssTnI: **none**

>*Galemys pyrenaicus TNNI1* (ssTnI)
MPEVERKSKITASRKLMLKSLMLAKAKECWEQEREEREAEKARYLAEHIPTLQTRGLSLRALQELCRDLHAKVEL
VDEERYDIEAKCLHNTREIKDLKLKVLDLRGKFKRPPLRRVRVSADAMLRALLGSKHKVSMDLRANLKSVKKEDT
EKERPVEVGDWRKNVEAMSGMEGRKKMFDAAKSPTSQ

Example MS/MS spectra corresponding to peptide: NIDALSGMEGR

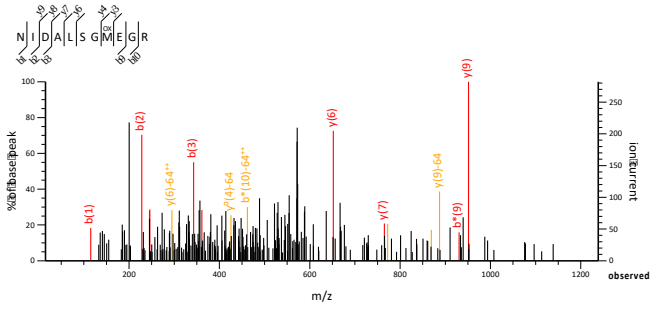

Figure S3. Liquid chromatography with tandem mass spectrometry (LC-MS/MS) protein sequencing on the ~22 kDa cardiac TnI bands from a Pyrenean desman (*Galemys pyrenaicus*) and a northern short-tailed shrew (*Blarina brevicauda*). Peptide matches to cTnI (*TNNI3*) are shown in red; no matches to ssTnI (*TNNI1*) were returned while peptide matches to other (non-TnI) protein products are not displayed.

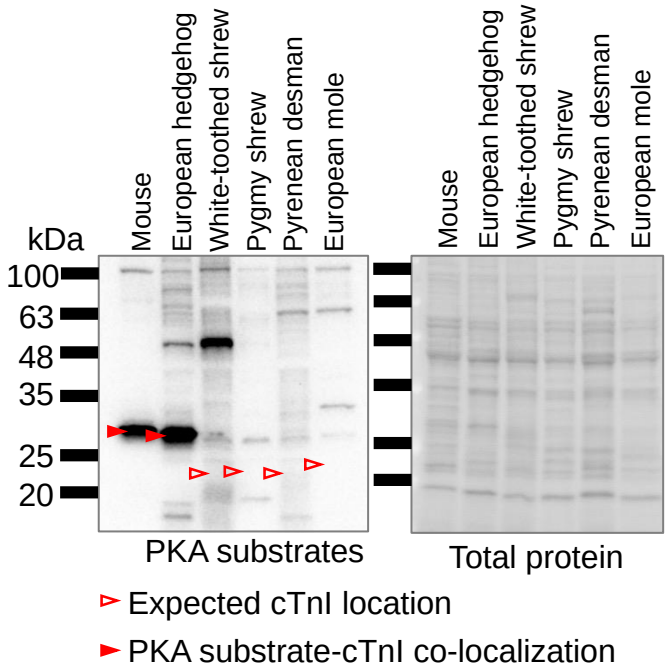

Figure S4. Total PKA phosphorylation of protein kinase A treated cardiac extracts from five eulipotyphlans and mouse. PKA targets were detected with a primary antibody (New England Biolabs 9624S) designed to identify phosphorylated serine (or threonine) with arginine at the -3 and -2 positions ("RRXS*/T*"). This includes the cardiac troponin I (cTnI) N-terminal extension as well as other unidentified PKA substrates. Red arrows indicate the expected position of cTnI (filled arrows show co-localised PKA substrate). For a blot on aliquots of the same samples with a phosho-cTnI specific antibody, see Fig. 1B.

Figure S5. Genomic DNA alignment illustrating the different mechanisms of *TNNI3* exon 3 inactivation in the talpid mole lineage. Mole species are denoted by asterisks; the two desman species with an intact exon 3 are underlined. The coding region of exon 3 is provided in uppercase letters, while the 5' and 3' flanking intron sequences are provided in lowercase letters. The acceptor ('ag') and donor ('gt') splice sites are shown in bold, with mutations in red font. The codons encoding the PKA phosphorylation site ($Ser_{23,24}$) in species with an intact exon 3 are presented in underlined italics. Frameshift deletions are highlighted in pink; a single frameshift insertion is highlighted in cyan; and a deletion that encompasses the intron 3-exon 3 boundary in *Talpa occidentalis* is highlighted in green. The *T. occidentalis* intron 3-exon 3 and upstream 10 bp deletions are also evident in a single read from the low coverage *T. europaea* SRA (SRR11679552) file (data S1).

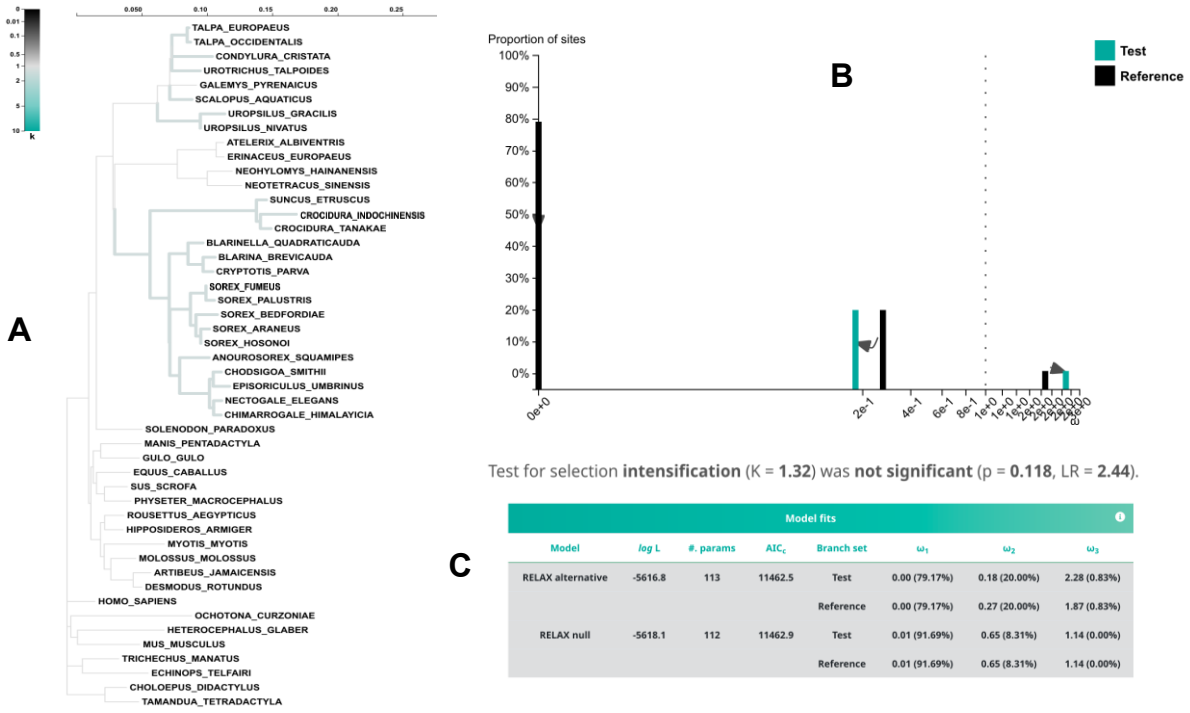

Figure S6. Selection analysis with *TNNI3* coding exons 1, 2, and 4-8 with 48 placental mammals. Analysis was performed with RELAX (*47*). The 'Test' or foreground category includes stem and crown soricid (shrew) branches and all stem and crown branches within Talpidae (moles) that have inactivating mutations (also see data S2). All other branches belong to the 'Reference' or background category. (A) Phylogenetic tree showing Test branches (thick lines) versus Reference branches (thin lines). The scale bar for the phylogenetic tree is in substitutions/site. The color of the Test branches corresponds to the scale bar for k in the upper left corner, where k is the selection intensity parameter. Further, k is the power to which ω for the Reference branches (ω_R) is raised so that it will be equal to ω for the Test branches (ω_T), that is, $\omega_T = \omega_R$. Selection on the Test branches can either be intensified (k > 1) or relaxed (k < 1) relative to the Reference branches, and the RELAX program uses a lnL ratio test to test for significance. (B) Omega plot showing ω values and frequencies for three classes of ω: ω1, ω2, and ω3. (C) Model fits for the NULL and RELAX models and results of the lnL test. There were no significant differences in selection between the two branch categories (p = 0.118).

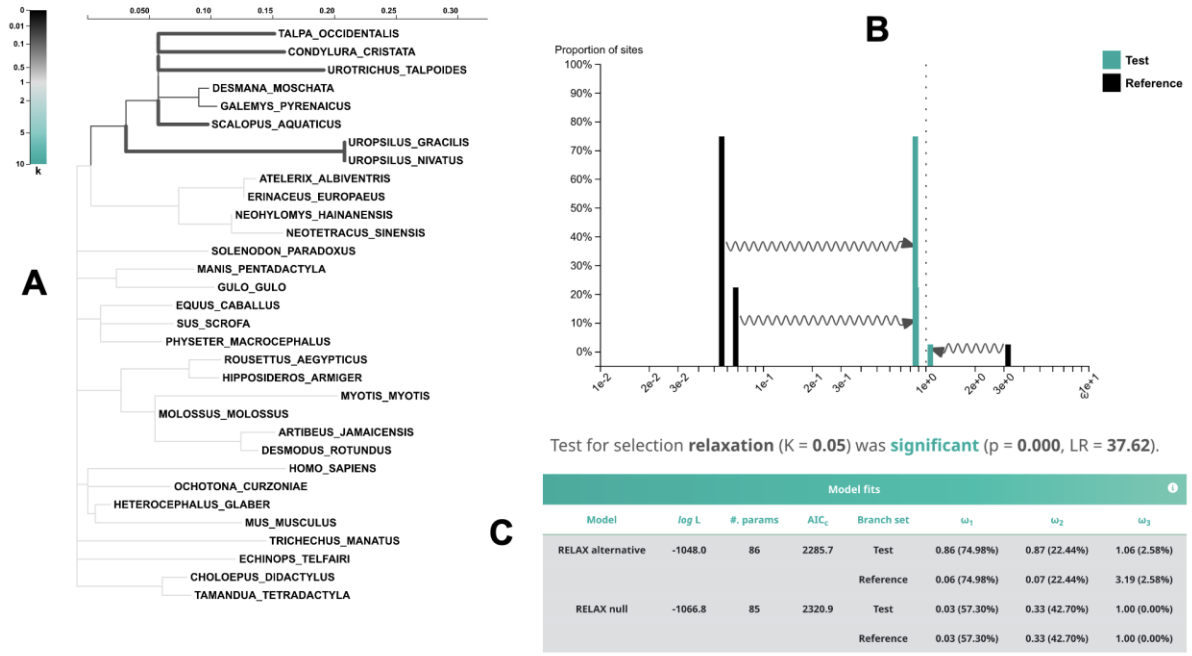

Figure S7. Selection analysis with *TNNI3* coding exons 3 with 32 placental mammals. Analysis was performed with RELAX (*47*). Sixteen shrews were not included in this analysis because any remnants of exon 3 were not recognizable. Inactivating frameshifts in talpid pseudoexons were filled in with Ns to restore complete codons. The 'Test' or foreground category includes all stem and crown branches within Talpidae (moles) that have inactivating mutations (also see Data S2). The 'Reference' or background category includes all non-talpid branches. This analysis also included Unclassified branches, which were excluded from the ω calculations and statistical comparison (also see data S2). (A) Phylogenetic tree showing Test branches (thick lines), Reference branches (thin, light lines), and Unclassified branches (thin, darker lines). The scale bar for the phylogenetic tree is in substitutions/site. The color of the Test branches corresponds to the scale bar for k in the upper left corner, where k is the selection intensity parameter. Further, k is the power to which ω for the Reference branches (ω_R) is raised so that it will be equal to ω for the Test branches (ω_T). Selection on the Test branches can either be intensified (k > 1) or relaxed (k < 1) relative to the Reference branches, and the RELAX program uses a lnL ratio test to test for significance. (B) Omega plot showing ω values and frequencies for three classes of ω: ω1, ω2, and ω3. (C) Model fits for the NULL and RELAX models and results of the lnL test. There was a significant difference in selection between the two branch categories ($p < 0.001$).

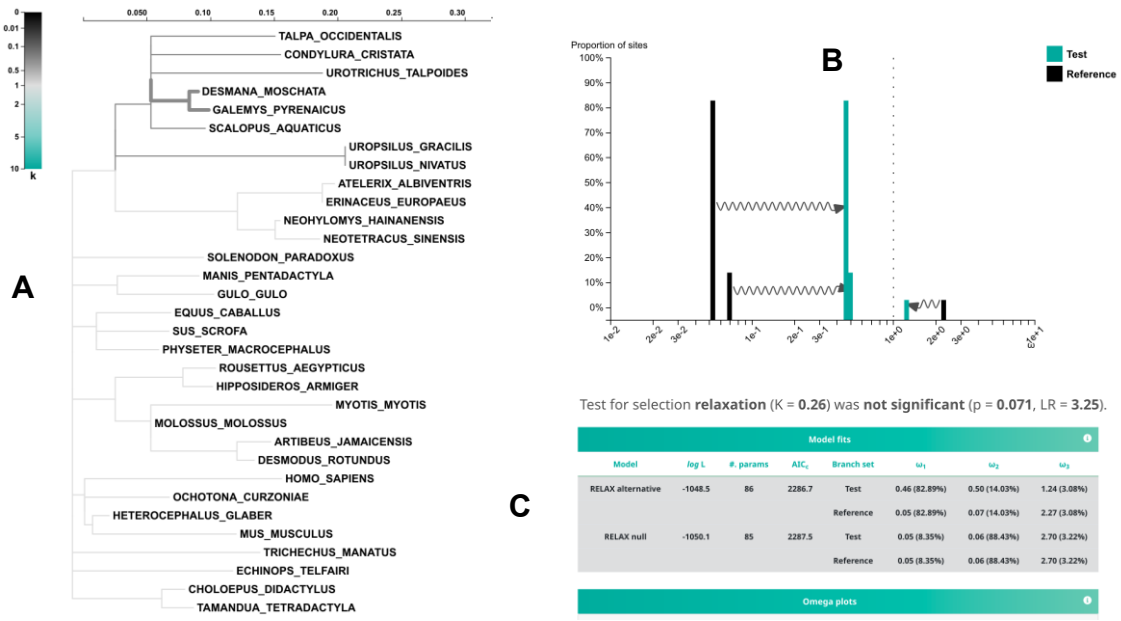

Figure S8. Selection analysis with *TNNI3* coding exons 3 with 32 placental mammals. Analysis was performed with RELAX (*47*). Sixteen shrews were not included in this analysis because any remnants of exon 3 were not recognizable. Inactivating frameshifts in talpid pseudoexons were filled in with Ns to restore complete codons. The 'Test' or foreground category includes both desmans (*Desmana*, *Galemys*) and their stem branch. The 'Reference' or background category includes all non-talpid branches. This analysis also included Unclassified branches, which were excluded from the ω calculations and statistical comparison (also see data S2). (A) Phylogenetic tree showing Test branches (thick lines), Reference branches (thin, light lines), and Unclassified branches (thin, darker lines). The scale bar for the phylogenetic tree is in substitutions/site. The color of the Test branches corresponds to the scale bar for k in the upper left corner, where k is the selection intensity parameter. Further, k is the power to which ω for the Reference branches (ω_R) is raised so that it will be equal to ω for the Test branches (ω_T). Selection on the Test branches can either be intensified (k > 1) or relaxed (k < 1) relative to the Reference branches, and the RELAX program uses a lnL ratio test to test for significance. (B) Omega plot showing ω values and frequencies for three classes of ω: ω1, ω2, and ω3. (C) Model fits for the NULL and RELAX models and results of the lnL test. There were no significant differences in selection between the two branch categories (p = 0.071).

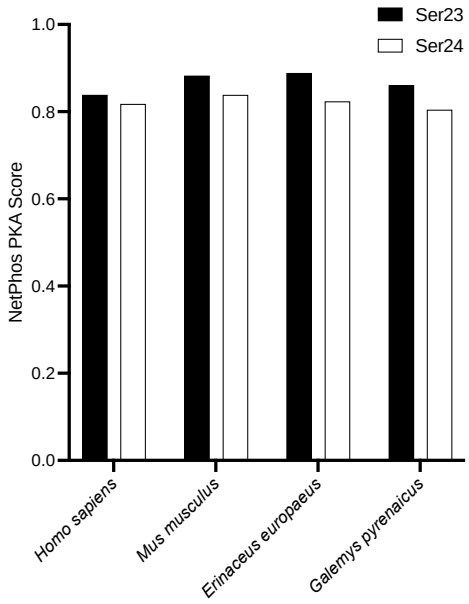

Figure S9. Protein kinase A (PKA) target scores for Ser$_{23}$ and Ser$_{24}$ (or equivalents) in human (*Homo sapiens*), mouse (*Mus musculus*), European hedgehog (*Erinaceus europaeus*) and Pyrenean desman (*Galemys pyrenaicus*). Scores were calculated with NetPhos 3.1 (*48*). Scores show if a given amino acid residue is predicted to be a target for a specific kinase, wherein values above 0.5 are considered 'positive' hits.

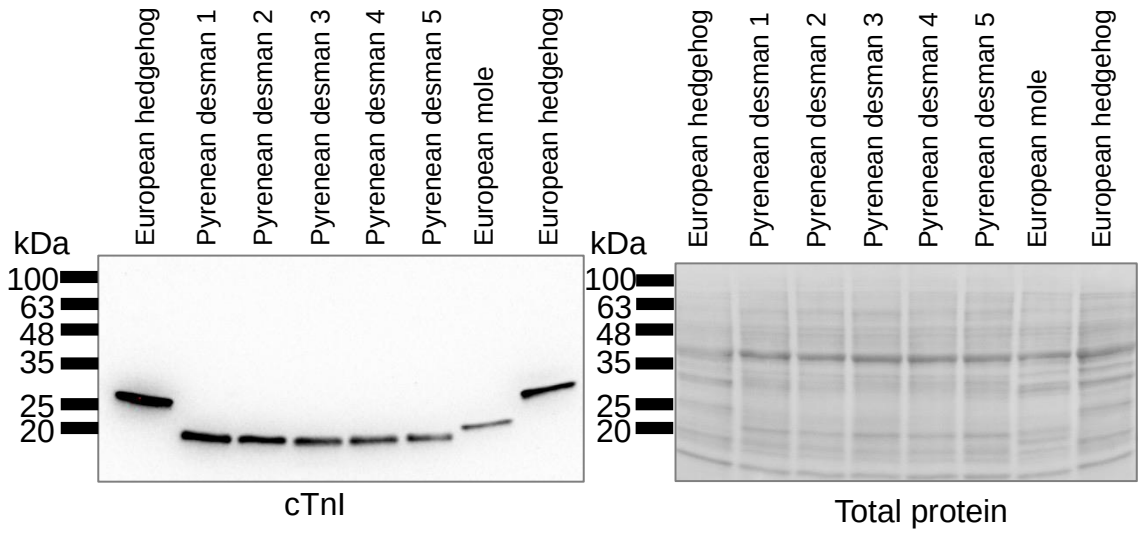

Figure S10. cTnI western blotting from five desman heart samples. Note that the same hedgehog sample was used in the two flanking lanes to provide an N-terminal extension-present standard. Two Pyrenean desman extracts (4 and 5) and the European mole were the same as used in panel fig. S2. Total protein was visualised with No-Stain Protein Labeling Reagent.

A


Hippisideros armiger
TNNI3 variant X1
Exon 1
Exon 2
Exon 3
Hippisideros armiger
TNNI3 variant X2
Exon 1
Exon 2
Exon 4
Exon 5

B

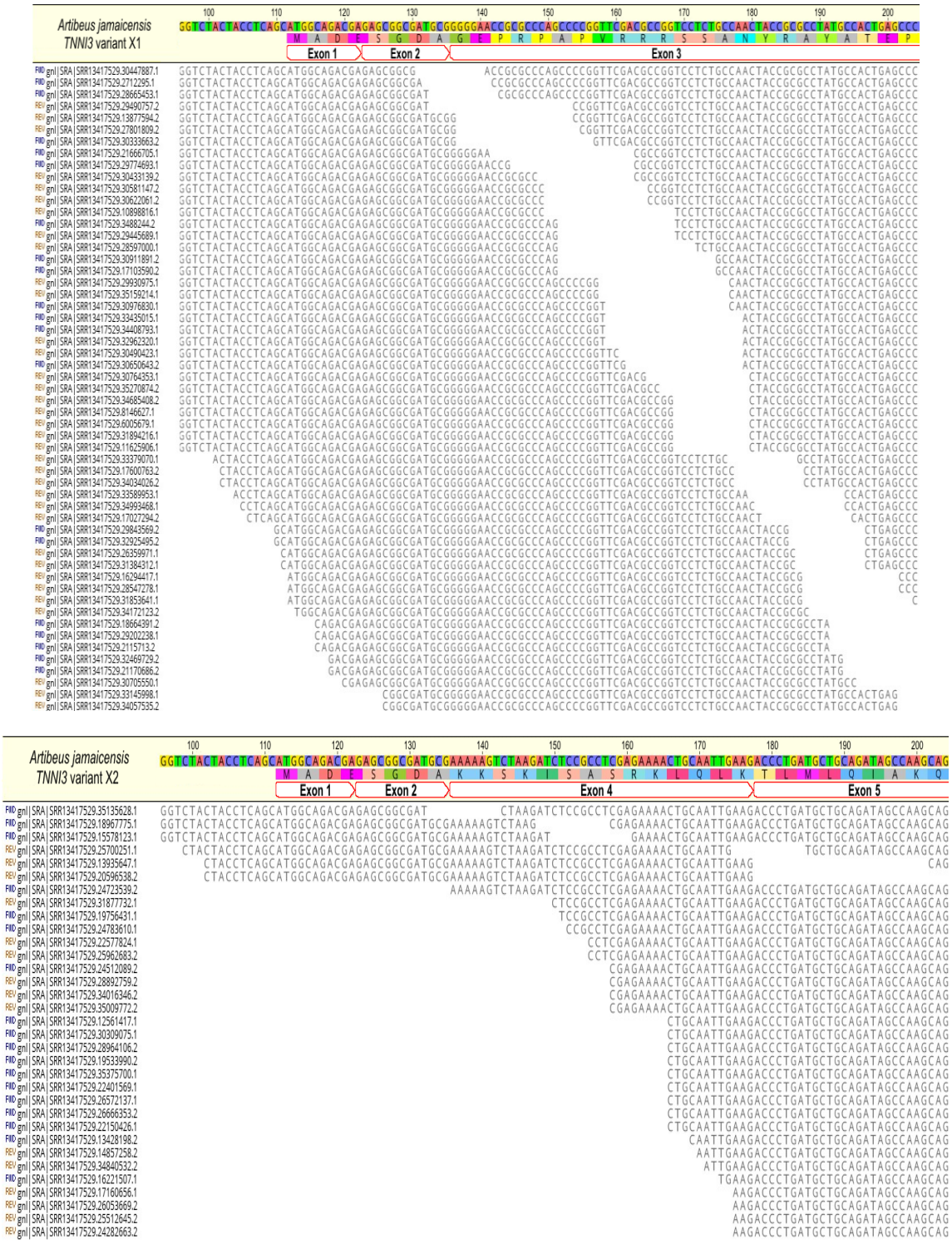

Figure S11. *TNNI3* heart transcriptome assemblies of two bat species illustrating the presence of two alternatively spliced variants. (A) *Hippisideros armiger* and (B) *Artibeus jamaicensis*. Note that the X2 variant of both species lacks exon 3.

A *Hipposideros armiger*

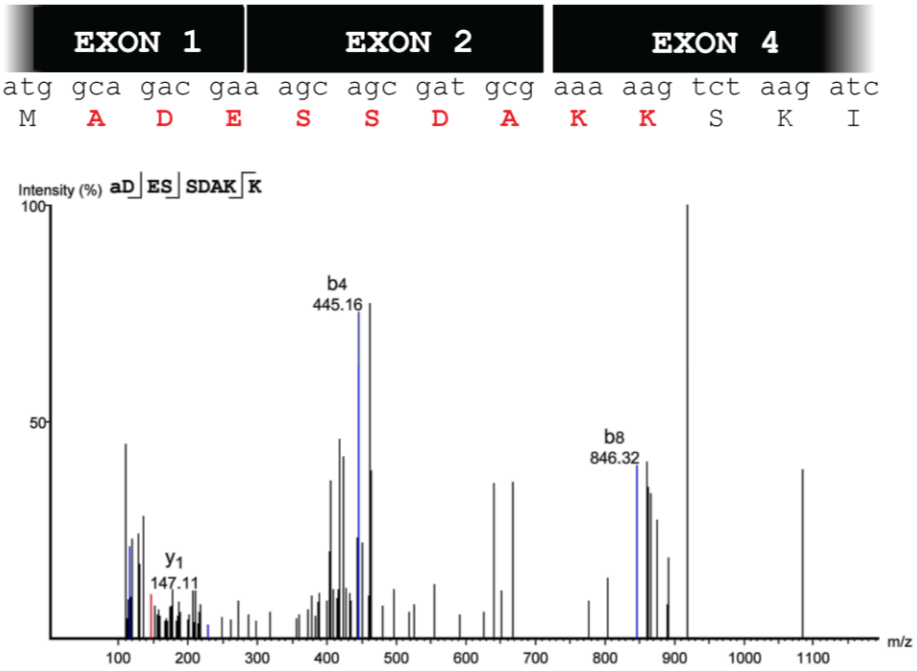

B *Suncus murinus*

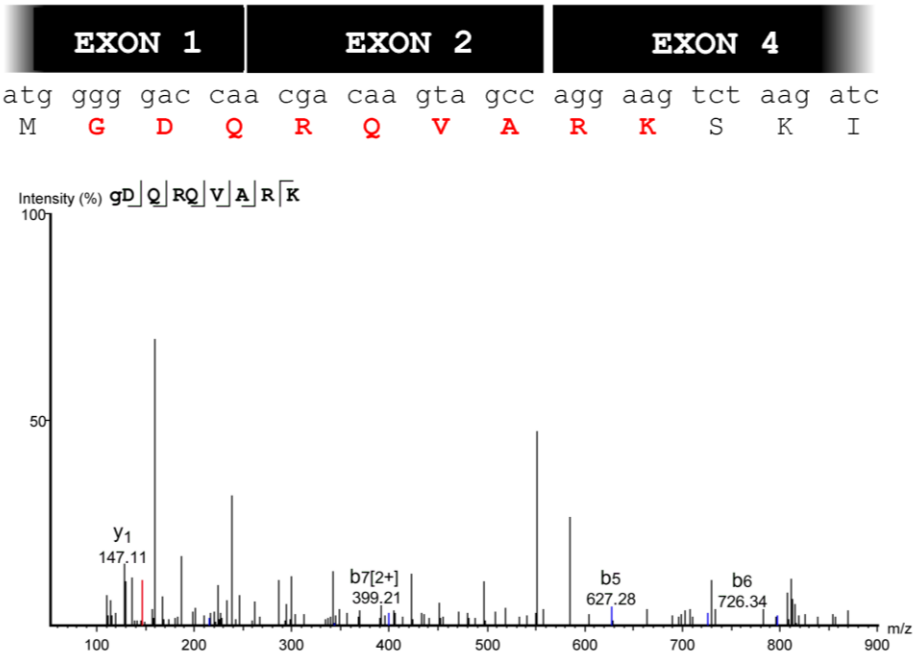

Figure S12. Liquid chromatography with tandem mass spectrometry (LC-MS/MS) protein sequencing with parallel reaction monitoring to identify N-terminal protein sequence in ~22 kDa cTnI bands from (A) great roundleaf bat (*Hipposideros armiger*) and (B) Asian house shrew (*Suncus murinus*). In both cases, peptides were identified that span *TNNI3* exons 1, 2 and 4, confirming that the splice variant lacking exon 3 is translated.

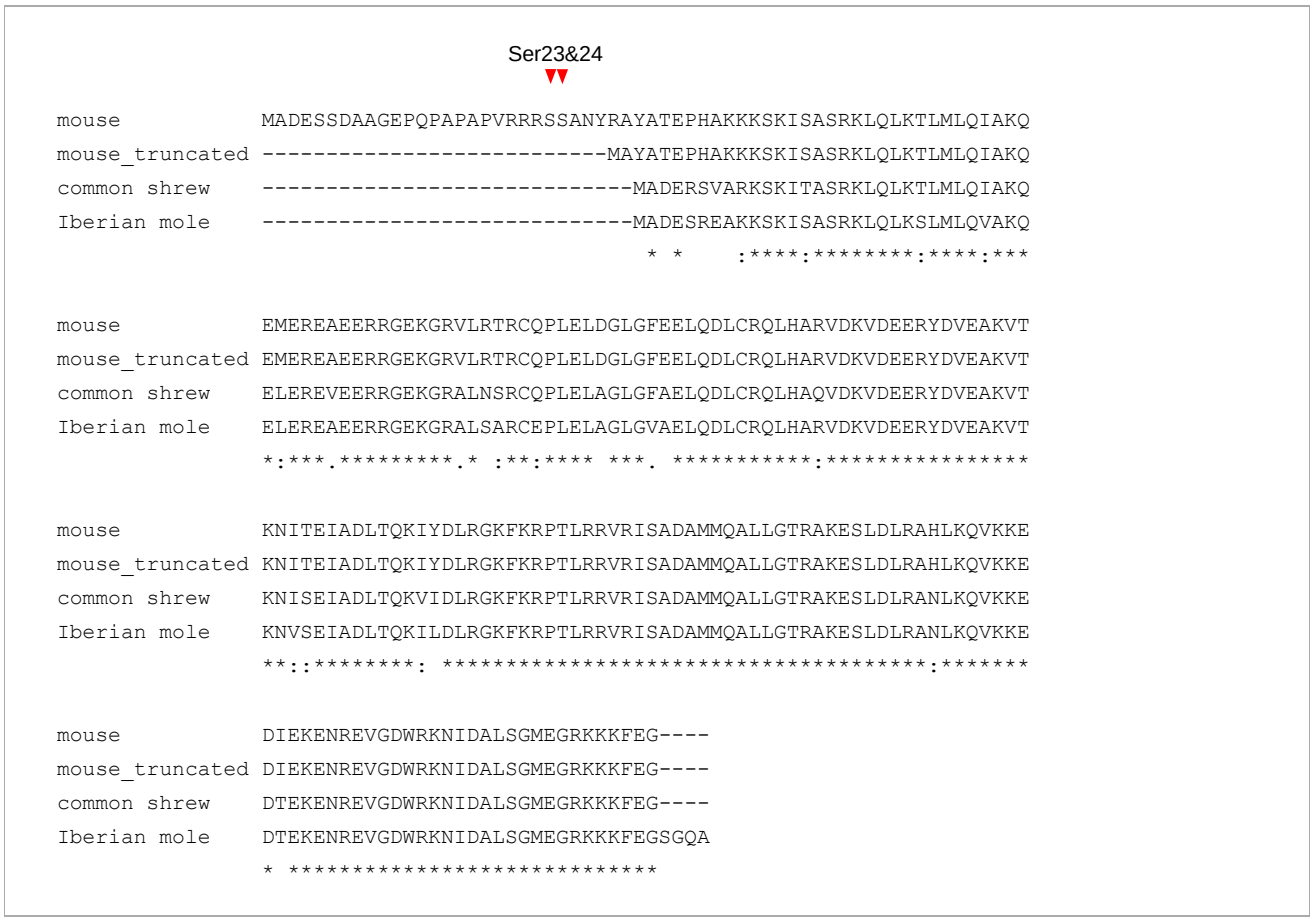

Figure S13. The genetic excision of exon 3 in *TNNI3* of shrews and moles recapitulates the truncated cardiac troponin I previously generated in transgenic mouse studies. The truncated mouse cTnI sequence is derived from Barbato et al. (2005) (*22*) who created a translation initiation codon before Ala_{29}. Shrews are represented by the common shrew, *Sorex araneus*, and moles are represented by the Iberian mole, *Talpa occidentalis* (see data S1 for sequence accession information). Red arrowheads denote the pertinent protein kinase A (PKA) target residues ($Ser_{23/24}$).

Species	Accession #	Sex/age	*TNNI3* hits	*TNNI1* hits
Eulipotyphla lacking *TNNI3* exon 3				
Sorex fumeus	SRR24416557	Male; ~2 months	66,004 (99.93%)	43 (0.07%)
Blarina brevicauda	SRR17216480	Unknown	128,824 (99.99%)	14 (0.01%)
Blarina brevicauda	SRR17216485	Unknown	91,832 (99.97%)	32 (0.03%)
Blarina brevicauda	SRR17216490	Unknown	110,629 (99.99%)	13 (0.01%)
Blarina brevicauda	SRR17216495	Unknown	70,094 (99.79%)	148 (0.21%)
Condylura cristata	SRR17216500	Unknown	71,859 (99.99%)	5 (0.01%)
Scalopus aquaticus	SRR17216400	Unknown	29,511 (99.24%)	227 (0.76%)
Scalopus aquaticus	SRR17216405	Unknown	10,541 (96.65%)	365 (3.35%)
Eulipotyphla possessing *TNNI3* exon 3				
Atelerix albiventris	SRR12442734	Male; adult	10,630 (71.7%)	4196 (28.3%)
Atelerix albiventris	SRR12442741	Female; adult	30,376 (96.91%)	970 (3.09%)
Chiroptera exhibiting alternative exon 3 splicing of *TNNI3*				
Hipposideros armiger	SRR1657902	Female; adult	48,370 (99.63%)	182 (0.27%)
Rhinolophus sinicus	SRR2273739	Male; adult	70,249 (99.88%)	87 (0.12%)
Rhinolophus clivosus	SRR13417526	Male; adult	67,669 (>99.99%)	1 (<0.01%)
Artibeus bogotensis	SRR13417527	Male; adult	123,547 (>99.99%)	6 (<0.01%)
Artibeus jamaicensis	SRR13417529	Male; adult	151,942 (99.95%)	78 (0.05%)
Artibeus jamaicensis	SRR13417530	Female; adult	150,160 (99.78%)	334 (0.22%)
Artibeus jamaicensis	SRR13417531	Male; adult	94,919 (99.51%)	465 (0.49%)
Artibeus jamaicensis	SRR13417532	Female; adult	185,058 (99.86%)	259 (0.14%)
Artibeus planirostris	SRR13417533	Male; adult	124,446 (99.96%)	56 (0.04%)
Artibeus fraterculus	SRR13417534	Male; adult	101,826 (99.73%)	278 (0.27%)

Table S1. Relative expression levels of *TNNI3* (cTnI) and *TNNI1* (ssTnI) for five eulipotyphlan and 7 chiropteran species. Expression levels for each gene were estimated by assembling publicly available heart transcriptomes for each species to exons 4-8 of *TNNI3* and exons 3-7 of *TNNI1*, respectively.

Species	Accession #	Sex/age	*TNNI3* FL hits	*TNNI3* AS hits
Hipposideros armiger	SRR1657902	Female; adult	7,611 (59.46%)	5,190 (40.54%)
Rhinolophus sinicus	SRR2273739	Male; adult	9,711 (57.69%)	7,121 (42.31%)
Rhinolophus clivosus	SRR13417526	Male; adult	9,155 (67.51%)	4,406 (32.49%)
Artibeus bogotensis	SRR13417527	Male; adult	11,813 (49.08%)	12,255 (50.92%)
Artibeus jamaicensis	SRR13417529	Male; adult	21,408 (65.58%)	11,234 (34.42%)
Artibeus jamaicensis	SRR13417530	Female; adult	26,001 (64.10%)	14,560 (35.90%)
Artibeus jamaicensis	SRR13417531	Male; adult	12,676 (62.09%)	7,740 (37.91%)
Artibeus jamaicensis	SRR13417532	Female; adult	25,232 (69.09%)	11,287 (30.91%)
Artibeus planirostris	SRR13417533	Male; adult	16,043 (65.00%)	8,637 (35.00%)
Artibeus fraterculus	SRR13417534	Male; adult	12,720 (67.57%)	6,105 (32.43%)

Table S2. Relative expression levels of full-length (possessing exon 3; '*TNNI3* FL') and alternatively spliced (lacking exon 3; '*TNNI3* AS') *TNNI3* transcripts for seven chiropteran species exhibiting alternative exon 3 splicing. Expression levels for each transcript were estimated by assembling publicly available heart transcriptomes for each species to 66 bp contigs (containing only exons 1, 2 and 4 for '*TNNI3* AS' and only exons 1, 2 and 42 bp of exon 3 for '*TNNI3* FL').

Latin name	Common name	Source	Other notes	Experiment
Mus musculus	House mouse (laboratory mouse).	Holly Shiels laboratory (University of Manchester, United Kingdom)	Figure 1B, S2, S4: C57BL/6 strain, male, 10 weeks old, wild-type (no genetic modifications). Sacrificed with cervical dislocation by trained personnel according to Home Office Schedule 1 regulations and with institutional approval (no specific project number applies as no experimental procedures were performed prior to euthanasia, as per UK regulations). Heart snap-frozen and stored at -80ºC.	Western blot
		Katinka Stecina laboratory (University of Manitoba, Canada)	Figure 1C: C57BL/6, female, 16 week-old Sim1CreTdTom-ChR2 mouse, anesthetized with isoflurane and heart surgically dissected out for protein extraction and storage at -65ºC. Animal use approved by the Local Animal User Committee of the University of Manitoba (Protocol #: Stecina lab; 20-003).	Western blot
		Guangdong Medical Laboratory Animal Center (Guangzhou, China)	Figure 4: C57BL/6 strain, female, 8 weeks old, wild-type (no genetic modifications). Euthanasia was performed by anesthesia with isoflurane and cervical dislocation. Heart tissue was frozen in liquid nitrogen and stored at -80ºC. Approved by Ethics Committee of Guangzhou University on Laboratory Animal Care (No.2023 -0071).	Western blot
Hipposideros armiger	Great roundleaf bat	Wenhua Yu (Guangzhou University, China)	Two specimens captured in Huizhou, Guangdong, China in July 2023. Euthanasia was performed by anesthesia with isoflurane and cervical dislocation. Heart tissue was frozen in liquid nitrogen and stored at -80ºC before western blotting. The fieldwork and sample collections were approved by the Department of Wildlife Protection, Guangdong Forestry Bureau and the Ethics Committee of Guangzhou University on Laboratory Animal Care (No. 2023 -0071).	Western blot, mass spectrometry analysis
Erinaceus europaeus	West *European hedgehog*	Private veterinary practice (United Kingdom)	Opportunistic tissue collection from a female juvenile euthanised by intrahepatic pentobarbital by veterinary surgeon. Animal had severe pneumonia secondary to lung worm infection and showed deteriorating health despite appropriate treatment with antiparaciticides (moxidectin/imidacloprid), antibiotic (enrofloxacin) and steroid (dexamethasone). Heart sample collected ~2 h post mortem. Heart preserved in RNAlater and stored at -80ºC.	Western blot, mRNA sequencing
Neotetracus sinensis	Shrew gymnure	Kai He (Guangzhou University, China)	One specimen captured at Mt. Ailaoshan, Yunnan, China in November 2019. Euthanasia was performed by cervical dislocation. Heart tissue preserved in RNAlater, and stored at -80ºC. The fieldwork and sample collections were approved by Ailaoshan Station for Subtropical Forest Ecosystem Studies and the administration bureaus of Jingdong Wuliangshan-Ailaoshan National Nature Reserve.	Transcriptome sequencing
Anourosorex squamipes	Chinese mole shrew	Kai He (Guangzhou University, China)	One specimen captured at Mt. Ailaoshan, Yunnan, China in November 2019. Euthanasia was performed by cervical dislocation. Heart tissue preserved in RNAlater, and stored at -80ºC before sequencing. The fieldwork and sample collections were approved by Ailaoshan Station for Subtropical Forest Ecosystem Studies and the administration bureaus of Jingdong Wuliangshan-Ailaoshan National Nature Reserve.	Transcriptome sequencing

			One specimen captured in Sichuan Normal University campus in June 2023. Euthanasia was performed by anesthesia with isoflurane and cervical dislocation. Heart tissue was frozen in liquid nitrogen and stored at -80ºC before western blotting. Sample collection was approved by Sichuan Normal University.	Western blot
Blarina brevicauda	Northern short-tailed shrew	Kevin Campbell (University of Manitoba, Canada)	One specimen obtained from Whiteshell Provincial Park in August 2005 under permission of a Government of Manitoba Conservation trapping permit (WB02279) and University of Manitoba approved Animal Use Protocol (F05-014). Specimen found dead in live trap and stored at -20°C.	Mass-spectrometry analysis
Blarinella quadraticauda	Asiatic short-tailed shrew	Kai He (Guangzhou University, China)	One specimen captured at Mt. Ailaoshan, Yunnan, China in November 2019. Euthanasia was performed by cervical dislocation. Heart tissue preserved in RNAlater, and stored at -80ºC. The fieldwork and sample collections were approved by Ailaoshan Station for Subtropical Forest Ecosystem Studies and the administration bureaus of Jingdong Wuliangshan-Ailaoshan National Nature Reserve.	Transcriptome sequencing
Chimarrogale himalayica varennei	Himalayan water shrew	Masaharu Motokawa (Kyoto University Museum, Japan)	Two specimens captured at Mt. Tay Con Linh, Ha Giang, Vietnam in March 2017. Heart tissue preserved in RNAlater, and stored at -80ºC. The fieldwork and sample collections were approved by Vietnam Academy of Science and Technology.	Transcriptome sequencing
Chodsigoa smithii	Smith's shrew	Kai He (Guangzhou University, China)	One specimen captured at Mt. Jinfoshan, Chongqing, China in November 2019. Euthanasia was performed by cervical dislocation. Heart tissue preserved in RNAlater, and stored at -80ºC. The fieldwork and sample collections were approved by the Jinfoshan National Nature Reserve.	Transcriptome sequencing
Crocidura russula	Greater white-toothed shrew	Killed by domestic cat (Valencia, Spain)	Opportunistic tissue collection from dead animal. Unconfirmed time of death, likely >24 h but not yet showing signs of decay. Estimated as 24 – 72 h post mortem. Heart preserved in RNAlater and stored at -80ºC.	Western blot, mRNA sequencing
Crocidura tanakae	Taiwanese gray shrew	Kai He (Guangzhou University, China)	One specimen captured at Mt. Chebaling, Guangdong China, December 2019. Euthanasia was performed by cervical dislocation. Heart tissue preserved in RNAlater, and stored at -80ºC. The fieldwork and sample collections were approved by the Chebaling National Nature Reserve and the Department of Wildlife Protection, Guangdong Forestry Bureau.	Transcriptome sequencing
Episoriculus umbrinus	Hidden brown-toothed shrew	Kai He (Guangzhou University, China)	One specimen captured at Mt. Ailaoshan, Yunnan, China in September 2019. Euthanasia was performed by cervical dislocation. Heart tissue preserved in RNAlater, and stored at -80ºC. The fieldwork and sample collections were approved by Ailaoshan Station for Subtropical Forest Ecosystem Studies and the administration bureaus of Jingdong Wuliangshan-Ailaoshan National Nature Reserve.	Transcriptome sequencing
Nectogale elegans	Elegant water shrew	Kai He (Guangzhou University, China)	One specimen captured at Mt. Wuliangshan, Yunnan, China. Euthanasia was performed by cervical dislocation. Heart tissue preserved in RNAlater, and stored at -80ºC. The fieldwork and sample collections were approved by Ailaoshan Station for Subtropical Forest Ecosystem Studies and the administration bureaus of Jingdong Wuliangshan-Ailaoshan National Nature Reserve.	Transcriptome sequencing

Sorex bedfordiae	Lesser striped shrew	Kai He (Guangzhou University, China)	One specimen captured at Mt. Ailaoshan, Yunnan, China. Euthanasia was performed by cervical dislocation. Heart tissue preserved in RNAlater, and stored at -80ºC. The fieldwork and sample collections were approved by Ailaoshan Station for Subtropical Forest Ecosystem Studies and the administration bureaus of Jingdong Wuliangshan-Ailaoshan National Nature Reserve.	Transcriptome sequencing
Sorex cinereus	Masked shrew	Kevin Campbell (University of Manitoba, Canada)	Three animals were captured in Winnipeg, Manitoba, Canada in October 2020 under permission of a Government of Manitoba Conservation trapping permit (WB24532) and cared for in accordance with the principles and guidelines of the Canadian Council of Animal Care (University of Manitoba Animal Use Protocol: F20-019 (AC11607)). Euthanasia performed by isoflurane overdose and heart stored at -80ºC.	mRNA sequencing
Sorex hosonoi	Azumi shrew	Kai He (Guangzhou University, China)	One specimen captured in the Shinshu University forest at Mt. Nishikoma, Nagano, Japan in October 2016. Euthanasia was performed by cervical dislocation. Heart tissue preserved in RNAlater, and stored at -80ºC. The fieldwork and sample collections were approved by Shinshu University Faculty of Agriculture.	Transcriptome sequencing
Sorex minutus	Eurasian pygmy shrew	Killed by domestic cat (West Yorkshire, United Kingdom)	Opportunistic tissue collection from dead animals. Two samples; one estimated to be <12 h post mortem, one <1 h post mortem. Heart preserved in RNAlater and stored at -80ºC.	Western blot
Sorex palustris	American water shrew	Kevin Campbell (University of Manitoba, Canada)	Two animals were captured at Nopiming Provincial Park, Manitoba, Canada in July 2020 under permission of a Government of Manitoba Conservation trapping permit (WB24532) and cared for in accordance with the principles and guidelines of the Canadian Council of Animal Care (University of Manitoba Animal Use Protocol: F20-019 (AC11607)). Euthanasia performed by isoflurane overdose and heart stored at -80ºC.	mRNA sequencing
Suncus murinus	House shrew	Kai He (Guangzhou University, China)	One specimen captured in Guangzhou, Guangdong China in July 2023. Euthanasia was performed by anesthesia with isoflurane and cervical dislocation. Heart tissue was frozen in liquid nitrogen and stored at -80ºC before western blot. The fieldwork and sample collections were approved by the Department of Wildlife Protection, Guangdong Forestry Bureau and by Ethics Committee of Guangzhou University on Laboratory Animal Care (No. 2023 -0071).	Western blot, mass spectrometry analysis
Desmana moschata	Russian desman	Anna Bannikova (Lomonosov Moscow State University, Russia)	Liver tissue sample (museum specimen: ZMMU S-181101) collected from Rackovskoye Lake, Vladimirskiy Region, Russia on August 25, 1993 and stored in ethanol at -20ºC. DNA previously extracted for unrelated studies (*38*, *39*). Permission for specimen collection was issued by The Ministry of Environment Protection and Natural Resources of the Russian Federation.	DNA sequencing
Dymecodon pilirostris	True's shrew mole	Kai He (Guangzhou University, China)	One specimen captured in the Shinshu University forest at Mt. Nishikoma, Nagano, Japan in October 2016. Euthanasia was performed by cervical dislocation. Heart tissue preserved in RNAlater, and stored at -80ºC. The fieldwork and sample collections were approved by Shinshu University Faculty of Agriculture.	Transcriptome sequencing
Galemys pyrenaicus	Pyrenean desman	Jorge González Esteban (DESMA	Opportunistic heart tissue collection from five dead specimens collected by environmental	Western blot, mRNA

		Estudios Ambientales, Spain)	consultant while conducting local government approved research (unrelated to the present study) in Navarra, Spain following national and international regulations. Specimens were stored at -20ºC for between 3 months and 12 years prior to sampling. Dissected hearts were placed in RNAlater and protein extracts stored at -80ºC.	sequencing, mass spectrometry analysis
Talpa europaea	European mole	Professional mole catcher using mechanical traps (West Yorkshire, United Kingdom)	Opportunistic tissue collection (pest control unrelated to scientific investigation). Two samples; both <18 h post-mortem and exhibiting rigor mortis. Heart preserved in RNAlater and stored at -80ºC.	Western blot, mRNA sequencing
Uropsilus gracilis	Gracile shrew-like mole	Kevin Campbell (University of Manitoba, Canada)	Liver tissue sample (museum specimen: KIZ211011) collected from dead female found in live trap on Mt. Laojun, Yunnan, China on August 19, 2001 and stored in ethanol at -20 ºC. Field work and sample collection was approved by the Laojun Mountain Administration Bureau, Yunnan, China. Specimen collected as part of another study (Shinohara et al. 2004 Zoological Science, 21(12):1177-1185).	DNA sequencing
		Kai He (Guangzhou University, China)	One specimen captured at Mt. Jinfoshan, Chongqing, China, in September 2019. Euthanasia was performed by cervical dislocation. Heart tissue preserved in RNAlater, and stored at -80ºC. The fieldwork and sample collections were approved by the Jinfoshan National Nature Reserve.	Transcriptome sequencing
Urotrichus talpoides	Greater Japanese shrew mole	Shin-ichiro Kawada (National Museum of Nature and Science, Japan).	Liver tissue sample (SIK207) collected from Higasi-nagura, Sitara town, Aichi Prefecture, Japan on June 5, 1999 and stored in ethanol at -20ºC. Fieldwork and sample collection was carried out in accordance with the guidelines of the Mammal Society of Japan	DNA sequencing
		Kai He (Guangzhou University, China)	One specimen captured in the Shinshu University forest at Mt. Nishikoma, Nagano, Japan in October 2016. Euthanasia was performed by cervical dislocation. Heart tissue preserved in RNAlater, and stored at -80oC. The fieldwork and sample collections were approved by Shinshu University Faculty of Agriculture.	Transcriptome sequencing

Table S3. Origins of samples used in this study.

Sample	Template	Forward primer	Reverse primer	Annealing temperature (°C)	Number of cycles
Sorex palustris	mRNA (cDNA)	TTTCTCTGCCTCCACAGCTC	CCTCAAACTTCTTCTTGCGG	55	30
Sorex cinereus	mRNA (cDNA)	TTTCTCTGCCTCCACAGCTC	CCTCAAACTTCTTCTTGCGG	55	30
Talpa europaea	mRNA (cDNA)	ATGGCGGACGAGAGCAGAGA	CCCTCGAACTTCTTCTTGCGG	66.1	30
Erinaceus europaeus	mRNA (cDNA)	TGGAACTCCTGATCTGATCG	TTTATTCCACAGGACCCTCTGG	60	30
Galemys pyrenaicus	mRNA (cDNA)	TTCCTCAGGCGCCGAAACG	CCTGCATCTTCGGGTCTGAGG	60.6	30
Desmana moschata	DNA	ATATTTAGTCTCTGTCCTGCC CACGGAGCCTCACGCCAAGGT	GCTGCAGCTTTCTTGAGG TGGGCCACCTGCAGCATCAG	58.4	30
Uropsilus gracilis	DNA	ATATTTAGTCTCTGCCCTCGCC AGGAGCAGAGATGCGGTGAG	TCAGCTGCAGTTTCCTTGAG TCCTTGAGGCCGAGATCTTAGG	70.0 70.0	30 30
Urotrichus talpoides	DNA	AGGAGCAGAGAAGCGGTGAG	TTCTTGAGGCGGAGATCTTAGAC	60.6	30

Table S4. List of primers and polymerase chain reaction conditions to amplify *TNNI3* from select eulipotyphlan species.

Supplementary Data

Data S1. List of species, *TNNI3* coding sequences, cTnI primary structures, and GenBank accession numbers associated with this study

Data S2. *TNNI3* selection analyses with codeml and RELAX

Data S3. Maximum entropy (MaxEnt) upstream (3´site of previous intron) and downstream (5´site of subsequent intron) splice site strength scoring for TNNI3 exons 2, 3 and 4.

Data S4. Densitometric analysis of *Hipposideros* cTnI western blots

References and Notes

1. D. M. Bers, Cardiac excitation-contraction coupling. *Nature* **415**, 198–205 (2002). doi:10.1038/415198a Medline

2. J. van der Velden, G. J. M. Stienen, Cardiac disorders and pathophysiology of sarcomeric proteins. *Physiol. Rev.* **99**, 381–426 (2019). doi:10.1152/physrev.00040.2017 Medline

3. S. Morimoto, Sarcomeric proteins and inherited cardiomyopathies. *Cardiovasc. Res.* **77**, 659–666 (2008). doi:10.1093/cvr/cvm084 Medline

4. P. M. Hwang, B. D. Sykes, Targeting the sarcomere to correct muscle function. *Nat. Rev. Drug Discov.* **14**, 313–328 (2015). doi:10.1038/nrd4554 Medline

5. P. J. M. Wijnker, A. M. Murphy, G. J. M. Stienen, J. van der Velden, Troponin I phosphorylation in human myocardium in health and disease. *Neth. Heart J.* **22**, 463–469 (2014). doi:10.1007/s12471-014-0590-4 Medline

6. G. S. Bodor, A. E. Oakeley, P. D. Allen, D. L. Crimmins, J. H. Ladenson, P. A. W. Anderson, Troponin I phosphorylation in the normal and failing adult human heart. *Circulation* **96**, 1495–1500 (1997). doi:10.1161/01.CIR.96.5.1495 Medline

7. H. J. Tadros, C. S. Life, G. Garcia, E. Pirozzi, E. G. Jones, S. Datta, M. S. Parvatiyar, P. B. Chase, H. D. Allen, J. J. Kim, J. R. Pinto, A. P. Landstrom, Meta-analysis of cardiomyopathy-associated variants in troponin genes identifies loci and intragenic hot spots that are associated with worse clinical outcomes. *J. Mol. Cell. Cardiol.* **142**, 118–125 (2020). doi:10.1016/j.yjmcc.2020.04.005 Medline

8. W. Joyce, D. M. Ripley, T. Gillis, A. C. Black, H. A. Shiels, F. G. Hoffmann, A revised perspective on the evolution of troponin I and troponin T gene families in vertebrates. *Genome Biol. Evol.* **15**, evac173 (2023). doi:10.1093/gbe/evac173 Medline

9. H. E. Salhi, V. Shettigar, L. Salyer, S. Sturgill, E. A. Brundage, J. Robinett, Z. Xu, E. Abay, J. Lowe, P. M. L. Janssen, J. A. Rafael-Fortney, N. Weisleder, M. T. Ziolo, B. J. Biesiadecki, The lack of troponin I Ser-23/24 phosphorylation is detrimental to in vivo cardiac function and exacerbates cardiac disease. *J. Mol. Cell. Cardiol.* **176**, 84–96 (2023). doi:10.1016/j.yjmcc.2023.01.010 Medline

10. B. J. Biesiadecki, K. Tachampa, C. Yuan, J.-P. Jin, P. P. de Tombe, R. J. Solaro, Removal of the cardiac troponin I N-terminal extension improves cardiac function in aged mice. *J. Biol. Chem.* **285**, 19688–19698 (2010). doi:10.1074/jbc.M109.086892 Medline

11. P. M. Hwang, F. Cai, S. E. Pineda-Sanabria, D. C. Corson, B. D. Sykes, The cardiac-specific N-terminal region of troponin I positions the regulatory domain of troponin C. *Proc. Natl. Acad. Sci. U.S.A.* **111**, 14412–14417 (2014). doi:10.1073/pnas.1410775111 Medline

12. J.-J. Sheng, J.-P. Jin, *TNNI1*, *TNNI2* and *TNNI3*: Evolution, regulation, and protein structure-function relationships. *Gene* **576**, 385–394 (2016). doi:10.1016/j.gene.2015.10.052 Medline

13. S. Marston, Recent studies of the molecular mechanism of lusitropy due to phosphorylation of cardiac troponin I by protein kinase A. *J. Muscle Res. Cell Motil.* **44**, 201–208 (2023). doi:10.1007/s10974-022-09630-4 Medline

14. D. M. Bers, Y. K. Xiang, M. Zaccolo, Whole-cell cAMP and PKA activity are epiphenomena, nanodomain signaling matters. *Physiology* **34**, 240–249 (2019). doi:10.1152/physiol.00002.2019 Medline

15. G. Ferrières, M. Pugnière, J. C. Mani, S. Villard, M. Laprade, P. Doutre, B. Pau, C. Granier, Systematic mapping of regions of human cardiac troponin I involved in binding to cardiac troponin C: N- and C-terminal low affinity contributing regions. *FEBS Lett.* **479**, 99–105 (2000). doi:10.1016/S0014-5793(00)01881-0 Medline

16. J. Wattanapermpool, X. Guo, R. J. Solaro, The unique amino-terminal peptide of cardiac troponin I regulates myofibrillar activity only when it is phosphorylated. *J. Mol. Cell. Cardiol.* **27**, 1383–1391 (1995). doi:10.1006/jmcc.1995.0131 Medline

17. S. Yasuda, P. Coutu, S. Sadayappan, J. Robbins, J. M. Metzger, Cardiac transgenic and gene transfer strategies converge to support an important role for troponin I in regulating relaxation in cardiac myocytes. *Circ. Res.* **101**, 377–386 (2007). doi:10.1161/CIRCRESAHA.106.145557 Medline

18. R. Zhang, J. Zhao, A. Mandveno, J. D. Potter, Cardiac troponin I phosphorylation increases the rate of cardiac muscle relaxation. *Circ. Res.* **76**, 1028–1035 (1995). doi:10.1161/01.RES.76.6.1028 Medline

19. W. Joyce, T. Wang, How cardiac output is regulated: August Krogh's proto-Guytonian understanding of the importance of venous return. *Comp. Biochem. Physiol. A Mol. Integr. Physiol.* **253**, 110861 (2021). doi:10.1016/j.cbpa.2020.110861 Medline

20. S. Marston, J. R. Pinto, Suppression of lusitropy as a disease mechanism in cardiomyopathies. *Front. Cardiovasc. Med.* **9**, 1080965 (2023). doi:10.3389/fcvm.2022.1080965 Medline

21. L. K. Gunther, H.-Z. Feng, H. Wei, J. Raupp, J.-P. Jin, T. Sakamoto, Effect of N-terminal extension of cardiac troponin I on the Ca^{2+} regulation of ATP-binding and ADP dissociation of myosin II in native cardiac myofibrils. *Biochemistry* **55**, 1887–1897 (2016). doi:10.1021/acs.biochem.5b01059 Medline

22. J. C. Barbato, Q.-Q. Huang, M. M. Hossain, M. Bond, J.-P. Jin, Proteolytic N-terminal truncation of cardiac troponin I enhances ventricular diastolic function. *J. Biol. Chem.* **280**, 6602–6609 (2005). doi:10.1074/jbc.M408525200 Medline

23. D. G. Ward, M. P. Cornes, I. P. Trayer, Structural consequences of cardiac troponin I phosphorylation. *J. Biol. Chem.* **277**, 41795–41801 (2002). doi:10.1074/jbc.M206744200 Medline

24. H.-Z. Feng, M. Chen, L. S. Weinstein, J.-P. Jin, Removal of the N-terminal extension of cardiac troponin I as a functional compensation for impaired myocardial β-adrenergic signaling. *J. Biol. Chem.* **283**, 33384–33393 (2008). doi:10.1074/jbc.M803302200 Medline

25. B. K. McConnell, Z. Popovic, N. Mal, K. Lee, J. Bautista, F. Forudi, R. Schwartzman, J.-P. Jin, M. Penn, M. Bond, Disruption of protein kinase A interaction with A-kinase-anchoring proteins in the heart in vivo: Effects on cardiac contractility, protein kinase A phosphorylation, and troponin I proteolysis. *J. Biol. Chem.* **284**, 1583–1592 (2009). doi:10.1074/jbc.M806321200 Medline

26. Z. B. Yu, L. F. Zhang, J. P. Jin, A proteolytic NH_2-terminal truncation of cardiac troponin I that is up-regulated in simulated microgravity. *J. Biol. Chem.* **276**, 15753–15760 (2001). doi:10.1074/jbc.M011048200 Medline

27. H.-Z. Feng, X. Huang, J.-P. Jin, N-terminal truncated cardiac troponin I enhances Frank-Starling response by increasing myofilament sensitivity to resting tension. *J. Gen. Physiol.* **155**, e202012821 (2023). doi:10.1085/jgp.202012821 Medline

28. C. M. Warren, M. Halas, H.-Z. Feng, B. M. Wolska, J.-P. Jin, R. J. Solaro, NH_2-terminal cleavage of cardiac troponin I signals adaptive response to cardiac stressors. *J. Cell. Signal.* **2**, 162–171 (2021). Medline

29. A. E. Messer, A. M. Jacques, S. B. Marston, Troponin phosphorylation and regulatory function in human heart muscle: Dephosphorylation of Ser23/24 on troponin I could account for the contractile defect in end-stage heart failure. *J. Mol. Cell. Cardiol.* **42**, 247–259 (2007). doi:10.1016/j.yjmcc.2006.08.017 Medline

30. Y. Li, P.-Y. J. Charles, C. Nan, J. R. Pinto, Y. Wang, J. Liang, G. Wu, J. Tian, H.-Z. Feng, J. D. Potter, J.-P. Jin, X. Huang, Correcting diastolic dysfunction by Ca^{2+} desensitizing troponin in a transgenic mouse model of restrictive cardiomyopathy. *J. Mol. Cell. Cardiol.* **49**, 402–411 (2010). doi:10.1016/j.yjmcc.2010.04.017 Medline

31. J. F. Shaffer, T. E. Gillis, Evolution of the regulatory control of vertebrate striated muscle: The roles of troponin I and myosin binding protein-C. *Physiol. Genomics* **42**, 406–419 (2010). doi:10.1152/physiolgenomics.00055.2010 Medline

32. M. Vornanen, Maximum heart rate of soricine shrews: Correlation with contractile properties and myosin composition. *Am. J. Physiol.* **262**, R842–R851 (1992). Medline

33. K. D. Jürgens, R. Fons, T. Peters, S. Sender, Heart and respiratory rates and their significance for convective oxygen transport rates in the smallest mammal, the Etruscan shrew *Suncus etruscus*. *J. Exp. Biol.* **199**, 2579–2584 (1996). doi:10.1242/jeb.199.12.2579 Medline

34. M. Vornanen, Basic functional properties of the cardiac muscle of the common shrew (*Sorex araneus*) and some other small mammals. *J. Exp. Biol.* **145**, 339–351 (1989). doi:10.1242/jeb.145.1.339 Medline

35. Y. H. Chang, B. I. Sheftel, B. Jensen, Anatomy of the heart with the highest heart rate. *J. Anat.* **241**, 173–190 (2022). doi:10.1111/joa.13640 Medline

36. P. Morrison, F. A. Ryser, A. R. Dawe, Studies on the physiology of the masked shrew *Sorex cinereus*. *Physiol. Zool.* **32**, 256–271 (1959). doi:10.1086/physzool.32.4.30155403

37. A. Nagel, The electrocardiogram of European shrews. *Comp. Biochem. Physiol. A Comp. Physiol.* **83**, 791–794 (1986). doi:10.1016/0300-9629(86)90729-2 Medline

38. K. He, T. G. Eastman, H. Czolacz, S. Li, A. Shinohara, S. I. Kawada, M. S. Springer, M. Berenbrink, K. L. Campbell, Myoglobin primary structure reveals multiple convergent transitions to semi-aquatic life in the world's smallest mammalian divers. *eLife* **10**, e66797 (2021). doi:10.7554/eLife.66797 Medline

39. K. He, A. Shinohara, K. M. Helgen, M. S. Springer, X.-L. Jiang, K. L. Campbell, Talpid mole phylogeny unites shrew moles and illuminates overlooked cryptic species diversity. *Mol. Biol. Evol.* **34**, 78–87 (2017). doi:10.1093/molbev/msw221 Medline

40. L. Saggin, L. Gorza, S. Ausoni, S. Schiaffino, Troponin I switching in the developing heart. *J. Biol. Chem.* **264**, 16299–16302 (1989). doi:10.1016/S0021-9258(18)71621-9 Medline

41. U. Oron, M. Mandelberg, Comparative morphometry of the mitochondria and activity of some enzymes in the myocardium of small mammals. *J. Mol. Cell. Cardiol.* **17**, 627–632 (1985). doi:10.1016/S0022-2828(85)80031-6 Medline

42. A. Armsby, T. Quilliam, H. Soehnle, Some observations on the ecology of the mole. *J. Zool.* **149**, 110–112 (1966). doi:10.1111/j.1469-7998.1966.tb02992.x

43. T. Allison, H. Van Twyver, Sleep in the moles, *Scalopus aquaticus* and *Condylura cristata*. *Exp. Neurol.* **27**, 564–578 (1970). doi:10.1016/0014-4886(70)90117-2 Medline

44. K. L. Campbell, P. W. Hochachka, Thermal biology and metabolism of the American shrew-mole, *Neurotrichus gibbsii*. *J. Mammal.* **81**, 578–585 (2000). doi:10.1644/1545-1542(2000)081<0578:TBAMOT>2.0.CO;2

45. K. L. Campbell, I. W. McIntyre, R. A. MacArthur, Fasting metabolism and thermoregulatory competence of the star-nosed mole, *Condylura cristata* (Talpidae: Condylurinae). *Comp. Biochem. Physiol. A Mol. Integr. Physiol.* **123**, 293–298 (1999). doi:10.1016/S1095-6433(99)00065-3 Medline

46. Z. Yang, PAML 4: Phylogenetic analysis by maximum likelihood. *Mol. Biol. Evol.* **24**, 1586–1591 (2007). doi:10.1093/molbev/msm088 Medline

47. J. O. Wertheim, B. Murrell, M. D. Smith, S. L. Kosakovsky Pond, K. Scheffler, RELAX: Detecting relaxed selection in a phylogenetic framework. *Mol. Biol. Evol.* **32**, 820–832 (2015). doi:10.1093/molbev/msu400 Medline

48. N. Blom, T. Sicheritz-Pontén, R. Gupta, S. Gammeltoft, S. Brunak, Prediction of post-translational glycosylation and phosphorylation of proteins from the amino acid sequence. *Proteomics* **4**, 1633–1649 (2004). doi:10.1002/pmic.200300771 Medline

49. G. Yeo, C. B. Burge, Maximum entropy modeling of short sequence motifs with applications to RNA splicing signals. *J. Comput. Biol.* **11**, 377–394 (2004). doi:10.1089/1066527041410418 Medline

50. P. J. Shepard, E.-A. Choi, A. Busch, K. J. Hertel, Efficient internal exon recognition depends on near equal contributions from the 3′ and 5′ splice sites. *Nucleic Acids Res.* **39**, 8928–8937 (2011). doi:10.1093/nar/gkr481 Medline

51. J.-J. Sheng, J.-P. Jin, Gene regulation, alternative splicing, and posttranslational modification of troponin subunits in cardiac development and adaptation: A focused review. *Front. Physiol.* **5**, 165 (2014). doi:10.3389/fphys.2014.00165 Medline

52. M. Rasmussen, J.-P. Jin, Troponin variants as markers of skeletal muscle health and diseases. *Front. Physiol.* **12**, 747214 (2021). doi:10.3389/fphys.2021.747214 Medline

53. The Human Protein Atlas, Tissue expression of TNNI3 – Summary; https://www.proteinatlas.org/ENSG00000129991-TNNI3/tissue.

54. F. M Real, S. A. Haas, P. Franchini, P. Xiong, O. Simakov, H. Kuhl, R. Schöpflin, D. Heller, M.-H. Moeinzadeh, V. Heinrich, T. Krannich, A. Bressin, M. F. Hartmann, S. A. Wudy, D. K. N. Dechmann, A. Hurtado, F. J. Barrionuevo, M. Schindler, I. Harabula, M. Osterwalder, M. Hiller, L. Wittler, A. Visel, B. Timmermann, A. Meyer, M. Vingron, R.

Jiménez, S. Mundlos, D. G. Lupiáñez, The mole genome reveals regulatory rearrangements associated with adaptive intersexuality. *Science* **370**, 208–214 (2020). doi:10.1126/science.aaz2582 Medline

55. J. R. Johnston, P. B. Chase, J. R. Pinto, Troponin through the looking-glass: Emerging roles beyond regulation of striated muscle contraction. *Oncotarget* **9**, 1461–1482 (2017). doi:10.18632/oncotarget.22879 Medline

56. S. Casas-Tintó, A. Maraver, M. Serrano, A. Ferrús, Troponin-I enhances and is required for oncogenic overgrowth. *Oncotarget* **7**, 52631–52642 (2016). doi:10.18632/oncotarget.10616 Medline

57. C. Chen, J.-B. Liu, Z.-P. Bian, J.-D. Xu, H.-F. Wu, C.-R. Gu, Y. Shi, J.-N. Zhang, X.-J. Chen, D. Yang, Cardiac troponin I is abnormally expressed in non-small cell lung cancer tissues and human cancer cells. *Int. J. Clin. Exp. Pathol.* **7**, 1314–1324 (2014). Medline

58. L. S. McRobb, V. S. Lee, M. Simonian, Z. Zhao, S. G. Thomas, M. Wiedmann, J. V. A. Raj, M. Grace, V. Moutrie, M. J. McKay, M. P. Molloy, M. A. Stoodley, Radiosurgery alters the endothelial surface proteome: Externalized intracellular molecules as potential vascular targets in irradiated brain arteriovenous malformations. *Radiat. Res.* **187**, 66–78 (2017). doi:10.1667/RR14518.1 Medline

59. P. B. Chase, M. P. Szczypinski, E. P. Soto, Nuclear tropomyosin and troponin in striated muscle: New roles in a new locale? *J. Muscle Res. Cell Motil.* **34**, 275–284 (2013). doi:10.1007/s10974-013-9356-7 Medline

60. J. R. Speakman, D. W. Thomas, "Physiological ecology and energetics of bats" in *Bat Ecology*, T. Kunz, M. Fenton, Eds. (Univ. Chicago Press, 2003), pp. 430–490.

61. D. K. N. Dechmann, S. Ehret, A. Gaub, B. Kranstauber, M. Wikelski, Low metabolism in a tropical bat from lowland Panama measured using heart rate telemetry: An unexpected life in the slow lane. *J. Exp. Biol.* **214**, 3605–3612 (2011). doi:10.1242/jeb.056010 Medline

62. M. T. O'Mara, M. Wikelski, C. C. Voigt, A. Ter Maat, H. S. Pollock, G. Burness, L. M. Desantis, D. K. Dechmann, Cyclic bouts of extreme bradycardia counteract the high metabolism of frugivorous bats. *eLife* **6**, e26686 (2017). doi:10.7554/eLife.26686 Medline

63. C. Zhu, Z. Chen, W. Guo, Pre-mRNA mis-splicing of sarcomeric genes in heart failure. *Biochim. Biophys. Acta Mol. Basis Dis.* **1863**, 2056–2063 (2017). doi:10.1016/j.bbadis.2016.11.008 Medline

64. S. E. Currie, G. Körtner, F. Geiser, Pronounced differences in heart rate and metabolism distinguish daily torpor and short-term hibernation in two bat species. *Sci. Rep.* **12**, 21721 (2022). doi:10.1038/s41598-022-25590-8 Medline

65. M. T. O'Mara, S. Rikker, M. Wikelski, A. Ter Maat, H. S. Pollock, D. K. N. Dechmann, Heart rate reveals torpor at high body temperatures in lowland tropical free-tailed bats. *R. Soc. Open Sci.* **4**, 171359 (2017). doi:10.1098/rsos.171359 Medline

66. S. M. Harrison, D. M. Bers, Influence of temperature on the calcium sensitivity of the myofilaments of skinned ventricular muscle from the rabbit. *J. Gen. Physiol.* **93**, 411–428 (1989). doi:10.1085/jgp.93.3.411 Medline

67. T. Veltri, G. A. P. de Oliveira, E. A. Bienkiewicz, F. L. Palhano, M. A. Marques, A. H. Moraes, J. L. Silva, M. M. Sorenson, J. R. Pinto, Amide hydrogens reveal a temperature-dependent structural transition that enhances site-II Ca^{2+}-binding affinity in a C-domain mutant of cardiac troponin C. *Sci. Rep.* **7**, 691 (2017). doi:10.1038/s41598-017-00777-6 Medline

68. B. Liu, L. C. Wang, D. D. Belke, Effects of temperature and pH on cardiac myofilament Ca^{2+} sensitivity in rat and ground squirrel. *Am. J. Physiol.* **264**, R104–R108 (1993). Medline

69. W. K. Milsom, M. B. Zimmer, M. B. Harris, Regulation of cardiac rhythm in hibernating mammals. *Comp. Biochem. Physiol. A Mol. Integr. Physiol.* **124**, 383–391 (1999). doi:10.1016/S1095-6433(99)00130-0 Medline

70. J. Taylor, "Evolution of energetic strategies in shrews" in *The Evolution of Shrews*, J. M. Wójcik, M. Wolsan, Eds. (Mammal Research Institute, Polish Academy of Sciences, 1998), pp. 309–346.

71. S. Engelhardt, L. Hein, F. Wiesmann, M. J. Lohse, Progressive hypertrophy and heart failure in β1-adrenergic receptor transgenic mice. *Proc. Natl. Acad. Sci. U.S.A.* **96**, 7059–7064 (1999). doi:10.1073/pnas.96.12.7059 Medline

72. K. Gao, A. Masuda, T. Matsuura, K. Ohno, Human branch point consensus sequence is yUnAy. *Nucleic Acids Res.* **36**, 2257–2267 (2008). doi:10.1093/nar/gkn073 Medline

73. J. Xie, L. Wang, R.-J. Lin, Variations of intronic branchpoint motif: Identification and functional implications in splicing and disease. *Commun. Biol.* **6**, 1142 (2023). doi:10.1038/s42003-023-05513-7 Medline

74. E. Lara-Pezzi, J. Gómez-Salinero, A. Gatto, P. García-Pavía, The alternative heart: Impact of alternative splicing in heart disease. *J. Cardiovasc. Transl. Res.* **6**, 945–955 (2013). doi:10.1007/s12265-013-9482-z Medline

75. A. Beqqali, Alternative splicing in cardiomyopathy. *Biophys. Rev.* **10**, 1061–1071 (2018). doi:10.1007/s12551-018-0439-y Medline

76. M. Gotthardt, V. Badillo-Lisakowski, V. N. Parikh, E. Ashley, M. Furtado, M. Carmo-Fonseca, S. Schudy, B. Meder, M. Grosch, L. Steinmetz, C. Crocini, L. Leinwand, Cardiac splicing as a diagnostic and therapeutic target. *Nat. Rev. Cardiol.* **20**, 517–530 (2023). doi:10.1038/s41569-022-00828-0 Medline

77. Z. Mahmud, S. Zahran, P. B. Liu, B. Reiz, B. Y. H. Chan, A. Roczkowsky, C. E. McCartney, P. L. Davies, L. Li, R. Schulz, P. M. Hwang, Structure and proteolytic susceptibility of the inhibitory C-terminal tail of cardiac troponin I. *Biochim. Biophys. Acta, Gen. Subj.* **1863**, 661–671 (2019). doi:10.1016/j.bbagen.2019.01.008 Medline

78. T. G. Martin, J. A. Kirk, Under construction: The dynamic assembly, maintenance, and degradation of the cardiac sarcomere. *J. Mol. Cell. Cardiol.* **148**, 89–102 (2020). doi:10.1016/j.yjmcc.2020.08.018 Medline

79. M. Rasmussen, H.-Z. Feng, J.-P. Jin, Evolution of the N-terminal regulation of cardiac troponin I for heart function of tetrapods: Lungfish presents an example of the emergence of novel submolecular structure to lead the capacity of adaptation. *J. Mol. Evol.* **90**, 30–43 (2022). doi:10.1007/s00239-021-10039-9 Medline

80. J. Kühnisch, C. Herbst, N. Al-Wakeel-Marquard, J. Dartsch, M. Holtgrewe, A. Baban, G. Mearini, J. Hardt, K. Kolokotronis, B. Gerull, L. Carrier, D. Beule, S. Schubert, D. Messroghli, F. Degener, F. Berger, S. Klaassen, Targeted panel sequencing in pediatric primary cardiomyopathy supports a critical role of *TNNI3*. *Clin. Genet.* **96**, 549–559 (2019). doi:10.1111/cge.13645 Medline

81. R. W. Meredith, J. E. Janečka, J. Gatesy, O. A. Ryder, C. A. Fisher, E. C. Teeling, A. Goodbla, E. Eizirik, T. L. L. Simão, T. Stadler, D. L. Rabosky, R. L. Honeycutt, J. J. Flynn, C. M. Ingram, C. Steiner, T. L. Williams, T. J. Robinson, A. Burk-Herrick, M. Westerman, N. A. Ayoub, M. S. Springer, W. J. Murphy, Impacts of the Cretaceous Terrestrial Revolution and KPg extinction on mammal diversification. *Science* **334**, 521–524 (2011). doi:10.1126/science.1211028 Medline

82. S. F. Altschul, T. L. Madden, A. A. Schäffer, J. Zhang, Z. Zhang, W. Miller, D. J. Lipman, Gapped BLAST and PSI-BLAST: A new generation of protein database search programs. *Nucleic Acids Res.* **25**, 3389–3402 (1997). doi:10.1093/nar/25.17.3389 Medline

83. M. J. Sullivan, N. K. Petty, S. A. Beatson, Easyfig: A genome comparison visualizer. *Bioinformatics* **27**, 1009–1010 (2011). doi:10.1093/bioinformatics/btr039 Medline

84. S. L. K. Pond, S. D. W. Frost, S. V. Muse, HyPhy: Hypothesis testing using phylogenies. *Bioinformatics* **21**, 676–679 (2005). doi:10.1093/bioinformatics/bti079 Medline

85. R. W. Meredith, J. Gatesy, W. J. Murphy, O. A. Ryder, M. S. Springer, Molecular decay of the tooth gene Enamelin (ENAM) mirrors the loss of enamel in the fossil record of placental mammals. *PLOS Genet.* **5**, e1000634 (2009). doi:10.1371/journal.pgen.1000634 Medline

86. A. J. Sabucedo, K. G. Furton, Estimation of postmortem interval using the protein marker cardiac troponin I. *Forensic Sci. Int.* **134**, 11–16 (2003). doi:10.1016/S0379-0738(03)00080-X Medline

87. M. S. Utter, C. M. Warren, R. J. Solaro, Impact of anesthesia and storage on posttranslational modifications of cardiac myofilament proteins. *Physiol. Rep.* **3**, e12393 (2015). doi:10.14814/phy2.12393 Medline

88. J. Kütt, G. Margus, L. Kask, T. Rätsepso, K. Soodla, R. Bernasconi, R. Birkedal, P. Järv, M. Laasmaa, M. Vendelin, Simple analysis of gel images with IOCBIO Gel. *BMC Biol.* **21**, 225 (2023). doi:10.1186/s12915-023-01734-8 Medline

89. Y. Wang, Y. Zhang, W. Hu, S. Xie, C.-X. Gong, K. Iqbal, F. Liu, Rapid alteration of protein phosphorylation during postmortem: Implication in the study of protein phosphorylation. *Sci. Rep.* **5**, 15709 (2015). doi:10.1038/srep15709 Medline

90. C. Natarajan, X. Jiang, A. Fago, R. E. Weber, H. Moriyama, J. F. Storz, Expression and purification of recombinant hemoglobin in *Escherichia coli*. *PLOS ONE* **6**, e20176 (2011). doi:10.1371/journal.pone.0020176 Medline